RESEARCH ARTICLE

Dietary intake of GDF11 delays the onset of several biomarkers of aging in male mice through anti-oxidant system via Smad2/3 pathway

Lili Song · Fei Wu · Congjun Li · Shicui Zhang

Abstract Current studies have generated controversy over the age-related change in concentration of growth differentiation factor 11 (GDF11) and its role in the genesis of rejuvenation conditions. In this study, we displayed rGDF11 on the surface of *Yarrowic Lipolytica* (*Y. lipolytica*), and proved the bioavailability of the yeast-displayed rGDF11 by oral delivery in aged male mice. On the basis of these findings, we started to explore the anti-aging activity and underlying mechanisms of displayed rGDF11. It was found that dietary intake of displayed rGDF11 had little influence on the body weight and biochemical parameters of aged male mice, but delayed the occurrence and development of age-related biomarkers such as lipofuscin (LF) and senescence-associated-β-galactosidase, and to some extent, prolonged the lifespan of aged male mice. Moreover, we demonstrated once again that dietary intake of displayed rGDF11 enhanced the activity of anti-oxidant enzymes, including catalase (CAT), superoxide dismutase (SOD) and glutathione peroxidase (GPX), reduced the reactive oxygen species (ROS) level, and slowed down the protein oxidation and lipid peroxidation. Importantly, we showed for the first time that rGDF11 enhanced the activity of CAT, SOD and GPX through activation of the Smad2/3 signaling pathway. Our study also provided a simple and safe route for delivery of recombinant GDF11, facilitating its therapeutic application in the future.

Keywords GDF11 · Yeast surface display · *Yarrowic Lipolytica* · Anti-aging · Lifespan

L. Song · F. Wu · C. Li · S. Zhang (✉)
Institute of Evolution & Marine Biodiversity and Department of Marine Biology, Ocean University of China, 5 Yushan Road, Qingdao 266003, China
e-mail: sczhang@ouc.edu.cn

S. Zhang
Laboratory for Marine Biology and Biotechnology, Qingdao National Laboratory for Marine Science and Technology, Qingdao 266003, China

Introduction

Growth differentiation factor 11 (GDF11) is a blood circulating protein of the transforming growth factor-β (TGF-β) family. It was identified in the heterochronic parabiosis as a potential antigeronic factor by Loffredo et al. (2013), and subsequently shown to play important roles in progression of aging and age-associated diseases (Walker et al. 2016). For example, many studies have shown that both expression of GDF11 gene and its protein abundance decline with age (Loffredo et al. 2013; Andersen and Lim 2014; Brack 2013; Hall 2014; Kaiser 2015; Katsimpardi et al. 2014; Zhou et al. 2016; Zhou et al. 2019a), and restoration of GDF11 reverses age-associated

cardiac hypertrophy, skeletal muscle dysfunction, hippocampal vascularity, and increases neural stem-cell proliferation (Loffredo et al. 2013; Katsimpardi et al. 2014; Zhou et al. 2016; Ozek et al. 2018; Sinha et al. 2014). Moreover, exogenous GDF11 treatment is able to improve tubular regeneration after acute kidney injury in elderly mice (Poggioli et al. 2016). However, these findings are questioned by some follow-up studies showing that human blood GDF11 exhibits little change or increases with age (Egerman et al. 2015; Rodgers and Eldridge 2015; Schafer et al. 2016; Smith et al. 2015), and GDF11 inhibits skeletal muscle regeneration (Egerman et al. 2015) and has no effect on cardiac aging-related cardiac hypertrophy (Smith et al. 2015). Additionally, GDF8 (myostatin), a closely related member of TGF-β superfamily, is highly homologous to GDF11, and is often perceived to serve similar or overlapping roles, further confusing the matters (Walker et al. 2016). Very recently, we have screened a highly specific anti-GDF11 antibody (sc-81952, Santa Cruz) which reacts with GDF11, and demonstrated that in fish and mouse, blood GDF11 abundance decreases with age (Zhou et al. 2019a, b). We have also shown that dietary intake of recombinant GDF11 (rGDF11) delays the development of age-related biomarkers, and even prolongs both the median and maximum lifespan of the annual fish *Nothobranchius guentheri* by enhancing antioxidant system. However, how GDF11 induces the enhancement of antioxidant system remains completely unknown.

Like other TGF-β superfamily members, GDF11 canonically binds to activin type II receptors (ActRIIA and ActRIIB), and then the complex recruits activin type I receptors (ALK4, ALK5 and ALK7), which in turn phosphorylates the intracellular signaling proteins Smad2 and Smad3 (McPherron et al. 1999; Patel and Amthor 2005; Rochette et al. 2015). Phosphorylated Smad2/3 associates with common mediator Smad4 and the Smad2/3/4 complex translocates to the nucleus where it mediates changes in gene expression (Walker et al. 2016; Andersen and Lim 2014; Katsimpardi et al. 2014; Andersson et al. 2006; Lebrun et al. 1999; Paul Oh et al. 2002). Recently, Yang et al. (2017) have shown that GDF11 administration increases the phosphorylation of Smad3 and decreases the phosphorylation of FOXO3a, which then affects ROS accumulation, suggesting a link between activation of Smad pathway by GDF11 and ROS accumulation. We wonder if GDF11 can enhance antioxidant system via the canonical Smad pathway during anti-aging process.

The method of yeast cell surface display, or simply, yeast display, has become a valuable protein engineering tool for a broad spectrum of biotechnology and biomedical/industrial applications (Cherf and Cochran 2015). Among the non-conventional yeasts, *Yarrowia lipolytica* Po1h with GRAS (Generally Recognized as Safe) status is one of the most attractive hosts for heterologous protein production owing to its unique characteristics that both the extracellular alkaline protease and extracellular acid protease genes have been deleted (Madzak et al. 2004). As GDF11 shows a great potential in rejuvenation and anti-aging applications, yeast-displayed GDF11 will certainly contribute to its utility as a therapeutic strategy. However, no yeast surface display of GDF11 has thus far been tried. In this study, GDF11 was displayed on the surface of *Y. lipolytica* via yeast surface display technology. In addition, the anti-aging activity and underlying mechanisms of the yeast-displayed GDF11 were explored using aged male mice as model. This study also provides a simple and safe route for delivery of recombinant GDF11, beneficial to its therapeutic application.

Materials and methods

Strains and plasmids

The host yeast for cell surface display *Yarrowic Lipolytica* (*Y. lipolytica*) Po1h (*MatA*, *ura3-302*, *xpr2-322*, *axp1-2*, *ΔAEP*, *ΔAXP*, *Suc⁺*) (Madzak et al. 2004) and the surface display vector pINA1317-YlCWP110 containing C-terminal end of *YlCWP110* from *Y. lipolytica* (Yue et al. 2008) were kindly donated by Dr. Zhenming Chi from the College of Marine Life Sciences, Ocean University of China. Based on the sequence of the fish *Nothobranchius guentheri* (*N. guentheri*) GDF11 gene (Zhou et al. 2019a), the cDNA encoding mature GDF11 with signal peptide deleted was amplified by PCR using the sense primer 5′-GGCCGTTCTGGCCGACGAGCCCAAT CTGCTG-3′ (SfiI site is underlined) and the antisense primer: 5′-GGATCCGTGATGGTGATGGTG ATGAGAGCAGCCACATCGATC-3′ (BamHI site is underlined and 6-His tag sequence is italicized). The

PCR product was digested with SfiI and BamHI, and sub-cloned into the plasmid pUC57-T simple vector previously cut with the same restriction enzymes. Ultimately, the cDNA ligated to pUC57-T simple vector was transformed into Trans5α *Escherichia coli* (*E. coli*). The transformants were incubated at 37 °C on Luria broth (LB) liquid medium with ampicillin (100 μg/ml) overnight, with a gentle shaking. The plasmids were extracted with E.Z.N.A Plasmid Mini Kit I (No: D6943-02; Omega Bio-tek) and sequenced. The plasmid constructed was named as pUC57-T simple-GDF11 and applied to the following experiments.

Construction of recombinant plasmid for yeast display of GDF11

The GDF11 display on the yeast cells of *Y. lipolytica* was performed as described by Yue et al. (2008). The plasmid pUC57-T simple-GDF11 was digested with SfiI at 50 °C overnight, followed by BamHI digestion at 37 °C for 3 h. The digests containing *gdf11* were recovered using E.Z.N.A. Gal Extraction Kit (No: D2500-02; Omega Bio-tek). The recovered products were ligated into the surface display vector pINA1317-YlCWP110 digested with the same enzymes and the recombinant plasmid carrying *gdf11* was designated pINA1317-GDF11-YlCWP110 (Supplementary Fig. 1). The recombinant plasmid was transformed into Trans5α *E. coli* and selected on the LB plates with kanamycin (50 μg/ml). The positive recombinant plasmid was extracted and purified as above. The recombinant plasmid pINA1317-GDF11-YlCWP110 purified was then digested with *Not*I. The linear fragments carrying *gdf11-YlCWP110* were recovered using E.Z.N.A. Gal Extraction Kit.

Transformation and selection

The *Y. lipolytica* Po1h was grown in 5 ml Yeast Extract Peptone Dextrose (YPD) medium (10 g/l yeast extract, 20 g/l bacto-peptone, 20 g/l glucose) and cultivated at 28 °C overnight. The suspension of the *Y. lipolytica* Po1h cells solution was transferred into 50 ml YPD medium and cultivated until the cell concentration reached about 2×10^7 cells/ml. The recovered linear fragments carrying *gdf11-YlCWP110* were transformed into *Y. lipolytica* by lithium acetate method (Xuan et al. 1988). The yeast cells transformed were spread on the Yeast Nitrogen

Base without Amino Acids (YNB) (1.7 g/l yeast nitrogen base without amino acids and ammonium sulfate, 10 g/l glucose, 5 g/l ammonium sulfate) plates, and cultivated at 28 °C for 96 h. *Y. lipolytica* Po1h cells carrying only *YlCWP110* without *gdf11* gene was used as control. A total of 100 colonies containing *gdf11-YlCWP110* fragment and 10 control colonies containing only *YlCWP110* were picked up from the YNB plates, and grown in 20 ml YPD liquid medium at 28 °C for 5 days, with a gentle shaking. The suspensions of the yeast cells were centrifuged at 3000×*g* at 4 °C for 15 min, and the pellets (yeast cells) collected for genomic DNA (gDNA) extraction.

gDNA extraction and polymerase chain reaction (PCR) detection

gDNA extraction of the yeast cells was performed as described by Borsenberger et al. (2018). The yeast cells carrying *YlCWP110* or *gdf11-YlCWP110* collected above were incubated in 300 μl of buffer T1 (Sorbitol 1 M; EDTA 0.1 M, pH8) with 5 μl of 10 mg/ml lyticase (dissolved with T1 buffer) (No: L4025; Sigma) at 37 °C for 15 min. After centrifugation, the yeast cell pellets were suspended in a lysis buffer (Tris 10 mM; EDTA 1 mM, pH8; NaCl 100 mM, Triton 2%; SDS 1%) with glass beads and phenol–chloroform-isoamyl alcohol (v/v/v, 25:24:1), vortexed for 2 min, and centrifuged. The supernatants were then precipitated with ethanol, and washed twice with ethanol 70%. The resulting DNA pellets were dissolved in 100 μl TE buffer with 1 μl RNase A (10 mg/ml), incubated at 37 °C for 15 min, and precipitated with ethanol. Finally, the gDNA was dissolved in sterile water and used for PCR.

To test if the *gdf11* gene has been integrated into the gDNA of *Y. lipolytica* Po1h, the primers (the forward primer was: 5′-GACGAGCCCAACCTGCTGCT-3′; the reverse primer was 5′-GGAGCAACCGCATCGGTCAAC-3′) and the gDNA obtained from the yeast cells carrying fragment *YlCWP110* or *gdf11-YlCWP110* were used for PCR. The PCR reaction was performed at 94 °C for 5 min, followed by 35 cycles of 94 °C for 30 s, 55 °C for 30 s, and 72 °C for 40 s. The PCR products were generated only from the gDNA of the yeast cells carrying *gdf11-YlCWP110*. We picked up 10 samples of PCR products at random for sequencing analysis (Sangon Biotech), and the results verified that *gdf11* was indeed integrated into

the gDNA of *Y. lipolytica* Po1h (data not shown). The *Y. lipolytica* Po1h carrying *gdf11-YlCWP110* were then used for immunofluorescence microscopy and protein sample preparation.

Immunofluorescence microscopy

The immunofluorescence microscopy was conducted as described by Pringle et al. (1991) using the anti His-tag mouse monoclonal antibody (No: CW0286; Cowin Bio) as primary antibody and fluorescein iso-thiocyanate (FITC)-conjugated goat anti-mouse IgG (immunoglobulin G) as secondary antibody (No: D110105; Sangon Biotech), respectively. Briefly, *Y. lipolytica* Po1h carrying *YlCWP110* or *gdf11-YlCWP110* were grown in YPD liquid medium at 28 °C for 5 days, with a gentle shaking. The cells were collected and washed three times with phosphate buffer saline (PBS). The *Y. lipolytica* Po1h pellets were suspended in 3.7% formaldehyde and incubated at 28 °C overnight with shaking. After centrifugation at $3000 \times g$ at 4 °C for 5 min, the yeast cells were collected and suspended in 250 μl PBS containing 1 mg/ml bovine serum albumin (BSA), and then 1.0 μl of anti His-tag mouse monoclonal antibody was added to the suspension. The mixture was incubated at 4 °C for 30 min. After washing with PBS three times, the yeast cells were re-suspended in 250 μl PBS containing 1 mg/ml BSA, and then 1 μl of secondary antibody was added to the suspension, and incubated under dark at 4 °C for 30 min. Finally, the labeled cells were observed under an Axio Scope A1 microscope (Carl Zeiss, Germany) with blue (450–490 nm) excitation light and 520 nm emission filters and photographed.

Yeast cells protein sample preparation

The total soluble fraction and cell wall fraction of yeast cells were prepared according to the method of Moon et al. (2013). In brief, *Y. lipolytica* Po1h carrying *YlCWP110* or *gdf11-YlCWP110* were grown in YPD liquid medium at 28 °C for 5 days, with a gentle shaking. The cells were collected and washed twice with chilled distilled water. For preparation of total soluble fraction, the yeast cells were suspended in TNE buffer (EDTA 0.5 M; NaCl 5 M; Tris–HCl 1 M, pH7.5) containing the protease inhibitors (0.5 mg/ml leupeptin, 0.5 mg/ml aprotinin,

0.7 mg/ml pepstatin, and 4 mg/ml phenylmethylsul-fonyl fluoride [PMSF]), and broken by vortexing with glass beads. After centrifugation at $16,000 \times g$ at 4 °C for 20 min, the supernatant was collected as total soluble fraction of yeast. For preparation of yeast cells wall fraction, the cell pellets were suspended in SDS/DTT extract solution (Tris–HCl 50 mM; EDTA 0.1 M, pH8.0; 2% SDS; DTT 10 mM). Both the total soluble fraction and cell wall fraction were used for Western blotting and enzyme-linked immunosorbent assay (ELISA).

Western blotting

Western blotting was performed as described by Dong et al. (2017). The yeast total soluble fraction and yeast cell wall fraction were electrophoresed on 12.5% acrylamide SDS-PAGE gels, and then transferred to polyvinylidene fluoride (PVDF) membranes. After blocking in 5% BSA (dissolved in 10 mM PBS (pH7.4)) at 25 °C for 1.5 h, the membranes were incubated with the primary antibodies against GDF11 (1:1000) (No. sc-81952; Santa Cruz Bio) and His-tag (1:1000) (No: CW0286; Cowin Bio), which were diluted with 10 mM PBS (pH7.4) containing 1% BSA, respectively. The membranes were then probed with corresponding secondary antibodies labeled with horseradish peroxidase (HRP) (1:6000) diluted with 10 mM PBS (pH7.4) containing 1% BSA. The bands were visualized by ECL Western blotting substrate (Thermo Fisher Scientific, USA).

Enzyme-linked immunosorbent assay

The rGDF11 expressed in *E. coil* transetta (DE3) was purified as described by Zhou et al. (2019a), and used to plot a standard curve. A sandwich enzyme-linked immunosorbent assay (ELISA) was performed to test the rGDF11 yield of per gram yeast cells and the total GDF11 concentration in serum of mice according to the method of Lim et al. (2015), with slight modification. Briefly, aliquots of 50 μl of GDF11-specific antibody (sc-81952; Santa Cruz Bio) diluted 1:500 with 10 mM PBS (pH7.4) was applied to each well of 96-well microplate, and air-dried at 4 °C overnight. The wells were each blocked with 200 μl of 10 mg/ml BSA in PBS at 37 °C for 2 h. After washing five times with 200 μl of PBS containing 0.5% Tween-20 (PBST), a total of 100 μl PBS containing 1 mg/

ml BSA plus different concentrations of rGDF11 (to calculate rGDF11 yield, the rGDF11 concentrations used for standard curve plotting were 0, 0.25, 0.5, 1, 2 and 4 µg/ml; and to calculate total GDF11 concentration in serum of mice, the rGDF11 concentrations used for standard curve plotting were 0, 100, 200, 500, 1000, 2000 pg/ml), total soluble fraction of yeast or serum of mice were added into each well, and incubated at 37 °C for 3 h. The wells were then washed five times with 200 µl of PBST, and incubated with 100 µl of biotin-binding GDF11 antibody (1:1000) (the biotinylation of GDF11 antibody was performed according to Lim et al. (2015)), diluted with 1 mg/ml BSA in PBS, at 37 °C for 1.5 h. After washing five times with PBST, the wells were further incubated with 100 µl of streptavidin-HRP (1:5000) and incubated at 37 °C for 1 h. The wells were washed several times with PBST and TMB substrate was added to each well, and incubated at 25 °C for 10–20 min in the absence of light. Finally, to stop the color development, 0.1 M HCl was added and the absorbances of the supernatants were measured at 450 nm under a Multiskan MK3 microplate reader (Thermo Fisher Scientific, USA). The rGDF11 yield of 1 g yeast cells and the total GDF11 concentration in serum of mice were calculated according to the standard curves (Supplementary Fig. 2a).

Animals, diet preparation and feeding

The treatment of experimental animals was in accordance with the guidelines of the Laboratory Animal Administration Law of China, with the permit number SCXK 20190003 approved by the Ethics Committee of the Laboratory Animal Administration of Shandong province. The specific pathogen-free male ICR mice (*Mus musculus*) aged 2.5 and 10 months (No. 1107262011002611) were purchased from Jinan Pengyue Laboratory Animal Breeding Co. Ltd., and housed one per cage in an environmentally controlled atmosphere (temperature 22 °C and relative humidity 56%) with a 12-h light/dark cycle. They were given free access to water and diet, and provided with shredded wood flour bedding. As the male ICR mice have a maximum lifespan of about 36 months, thus 3-month-old and 24-month-old male ICR mice were used as models of young and aged mice (Fujitsuka et al. 2016; Hunsche et al. 2016), respectively.

The diets were prepared as below. The ELISA showed that the transformant T46 has the highest rGDF11 yield of approximately 2.168 µg/g *Y. lipolytica* Po1h (Supplementary Table 1; Fig. 1d), and thus T46 yeast strain was cultivated in large scale (in YPD liquid medium at 28 °C for 5 days with gentle shaking) for diet preparation. In parallel, *Y. lipolytica* Po1h cells harboring *YlCWP110* only was also cultivated for control. The suspensions of yeast cells were centrifuged at 5000×*g* at 4 °C for 15 min, and the pellets were washed three times with PBS, and collected for diet preparation. Solid mice chow (normal diet: complete semisynthetic columnar-formed diet containing 18% crude proteins and 5% cellulose following the Chinese Association for Laboratory Animal Sciences) was smashed by the multifunctional disintegrator (Yongkang Red Sun Electromechanical Co. LTD), and the powdered chow equally divided into several portions (about 4 g powdered chow per portion). Each portion of powdered chow was mixed with 3.7 g *Y. lipolytica* Po1h cells harboring rGDF11-YlCWP110, which contained about 8 µg rGDF11 (the rGDF11 was at a dose of 0.2 mg/kg body weight) or *Y. lipolytica* Po1h cells harboring YlCWP110 only, and frozen at − 20 °C till use. Normal diet mixed with *Y. lipolytica* Po1h cells harboring rGDF11-YlCWP110 was named as experimental diet, and normal diet mixed with *Y. lipolytica* Po1h cells harboring YlCWP110 named as control diet.

Young male mice (3 months old; n = 8) were given free access to the normal diet and drinking water for 1 month. Aged male mice (24 months old; n = 48) were at random divided into 3 groups (16 individuals per group). Each mouse in group 1 (AMG1) was allowed free access to the normal diet and drinking water for 1 month; each mouse in group 2 (AMG2) fed with one piece of control diet per day, and then allowed free access to the normal diet and drinking water for 1 month; and each mouse in group 3 (AMG3) fed with one piece of experimental diet per day, and then allowed free access to the normal diet and drinking water for 1 month. During the experimental period, the body weight of each mouse in all groups was measured every 7 days, and recorded. At the end of experiments, 8 individuals of aged male mice were sampled from groups 1, 2 and 3 respectively, anesthesized by intraperitoneal injection of 3% pentobarbital at a dose of 2 ml/kg of body weight (Song et al. 2020a),
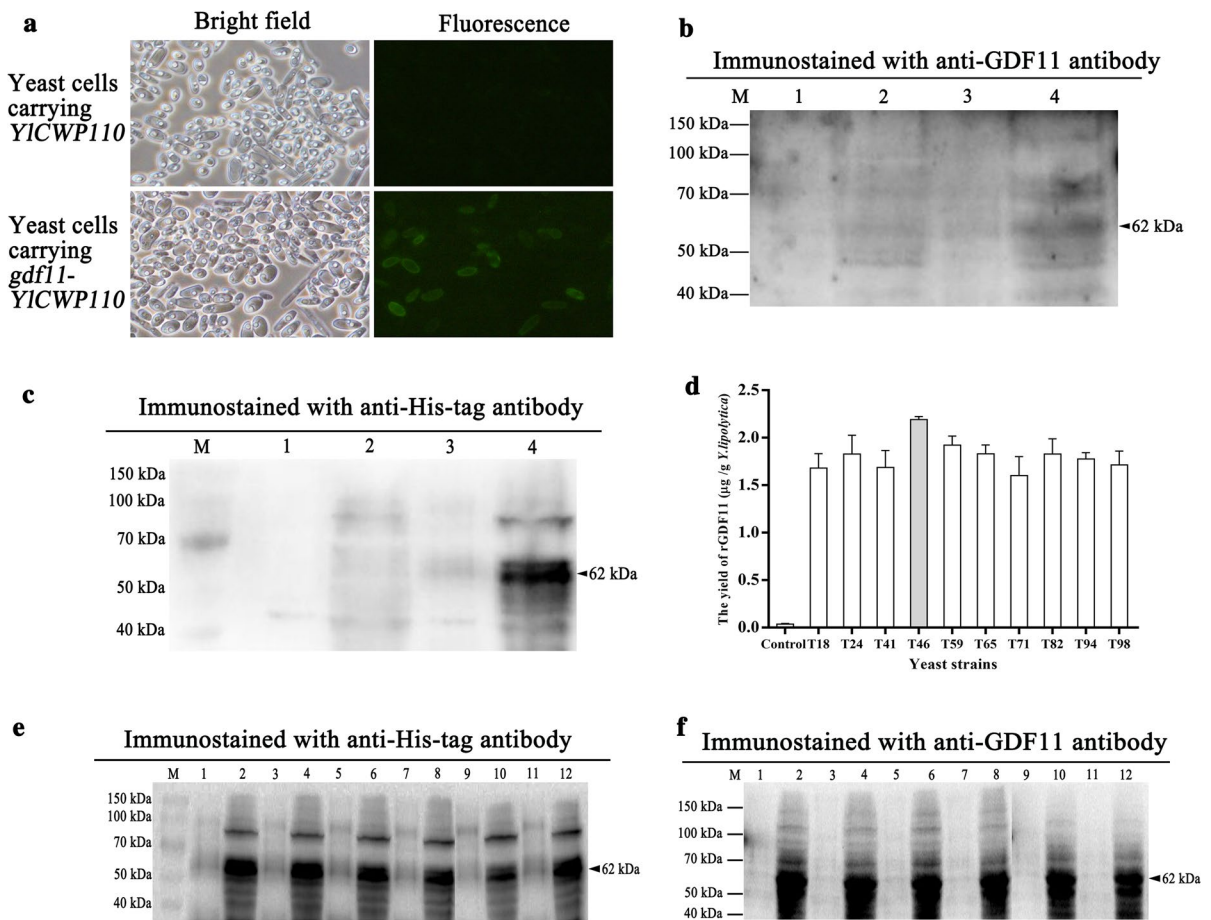
Fig. 1 Surface display of rGDF11 on *Y. lipolytica*. **a** The immunofluorescent labeling of the transformed *Y. lipolytica* cells using His-tag mouse monoclonal antibody as the primary antibody and IgG/FITC as the secondary antibody. The microphotographs were taken under bright light, and immunofluorescence microphotographs were taken under emission at 550 nm. Magnification: 40×10; **b** Western blotting of rGDF11 using mouse anti-GDF11 antibody as the primary antibody; **c** Western blotting of rGDF11 using His-tag mouse monoclonal antibody as the primary antibody. Lane M: marker; line 1 and line 3: the cell wall fraction of yeast cells carrying fragment *YlCWP110* or *gdf11-YlCWP110*, line 2 and line 4: the total soluble fraction of yeast cells carrying fragment *YlCWP110* or *gdf11-YlCWP110*; **d** The rGDF11 yield of the different strains (ten of 100 transformants). The control: *Y. lipolytica* Po1h only carrying YlCWP110; **e** western blotting was used to test the stability of rGDF11 expression and display, His-tag mouse monoclonal antibody was used as the primary antibody; **f** western blotting was used to test the stability of rGDF11 expression and display, mouse anti-GDF11 antibody was used as the primary antibody. Lane M: marker; line 1, 3, 5, 7, 9, 11: the cell wall fraction from each generation of yeast cells carrying rGDF11-Y1CWP110, line 2, 4, 6, 8, 10, 12: the total soluble fraction of yeast cells carrying fragment rGDF11-Y1CWP110. Date represent mean ± standard deviation (SD) (n = 3)

and the blood was collected from heart, and the livers and kidneys were dissected out of mice for the following experiments. Similarly, the young male mice were anesthesized by intraperitoneal injection of 3% pentobarbital at a dose of 2 ml/kg of body weight, and the blood was collected from heart, and the livers and kidneys were dissected out. The remaining 8 individuals of aged male mice in each group were continuously cultured for survivorship assay.

Blood sampling, serum preparation and biochemical parameter assay

Blood was collected from each mouse of AMG3 by bleeding of tail vein prior to the feeding of

experimental diet and at 6 h after the first-time feeding of experimental diet. Serum was prepared from the blood samples by centrifugation at 3000×g at 4 °C for 15 min, stored at −80 °C and used for Western blotting as described above. Blood was also collected from heart of each mouse of young group, AMG1, AMG2 and AMG3 at the end of feeding experiment, and serum was prepared as above. The serum was divided into two parts: one part was used for ELISA assay and the following experiments, and the other part was used for assay of biochemical parameters including total protein (TP), albumin (ALB), globulin (GLO), alanine transaminase (ALT), aspartate transferase (AST), total bilirubin (TBIL), direct bilirubin (DBIL), indirect bilirubin (IBIL), triglyceride (TG), total cholesterol (TC), high-density lipoprotein (HDL), low-density lipoprotein (LDL), blood urea nitrogen (BUN), creatinine (CREA) and uric acid (UA) using an automatic biochemistry analyzer (Hitachi P7600).

Survivor assay

The health of each aged male mouse in AMG1, AMG2 and AMG3 was surveilled every day. The survival of the mice was recorded until death of all the mice. The deaths occurring with period of 1 month were totaled for statistical calculations and represented one point in the survival curves (Kunstyr and Leuenberger 1975). The maximum and mean lifespan were calculated by the method of Markofsky and Perlmutter (1973). The commercially available Graph-Pad Prism 7 program was used to draw the survival curves of the three groups.

RNA isolation, cDNA synthesis and semi-quantative real-time PCR

The RNAs were extracted from the livers and kidneys of the mice with RNAiso plus (TaKaRa). The cDNAs were synthesized with Prime-Script™ RT reagent Kit with gDNA Eraser (TaKaRa) according to the manufacturer's instructions, and stored at −20 °C until use. The expression of mice-*cat* (NM_009804.2), mice-*sod* (NM_011434.2), and mice-*gpx* (BC086649.1) were examined by qRT-PCR. Primer Premier 5.0 program was used to design the specific primers of each gene (Supplementary Table 2). The mice-*gapdh* (GU214026.1)

gene was chosen as the reference for internal standardization. The amplification efficiency of each primer set was assessed using the liver cDNAs diluted twofold serially (Supplementary Table 3). The amplification was performed on ABI 7500 real-time PCR system (Applied Biosystems) at 95 °C for 10 s, followed by 40 cycles of 95 °C for 5 s, 60 °C for 15 s, and 72 °C for 35 s. The expression levels of *cat*, *sod* and *gpx* relative to that of *gapdh* were calculated by the comparative CT method ($2^{-\Delta\Delta CT}$).

Histological observation

The livers and kidneys dissected out of the mice were fixed in 4% paraformaldehyde at 4 °C for 12 h. After dehydration, both the tissues were embedded in optical cutting temperature compound, and cryo-sectioned at a thickness of 12 μm under −20 °C (Leica, Germany). For lipofuscin (LF) detection, the un-stained sections of the livers and kidneys were viewed under an Axio Scope A1 microscope (Carl Zeiss, Germany) with blue (450–490 nm) excitation light and 520 nm emission filters. For senescence-associated-β-galactosidase (SA-β-Gal) detection, the sections of livers and kidneys were washed with PBS, stained at 37 °C for 12 h by immersion in SA-β-Gal stain solution, and observed under Axio Scope A1 microscope with bright-field (Liu et al. 2015). The areas of LF fluorescence and SA-β-Gal staining area were determined using Image J software.

Assay for reactive oxygen species (ROS)

The livers and kidneys dissected out of the mice were homogenized using Polytron and sonicator in 50 mM PBS (pH7.4). The homogenates were centrifuged at 5000×g at 4 °C for 10 min, and the supernatants pooled. The protein concentration of the supernatants was determined with a BCA Protein Assay Kit (No: CW0014; CWBIO) (Song et al. 2020b). The dichloro-dihydro-fluorescein diacetate (DCFH-DA), a reagent for ROS quantitative determination (No. S0033S; Beyotime), was used in this study. The fluorescence intensity was monitored at an excitation wavelength of 488 nm and an emission wavelength of 525 nm under a GENios Plus spectrofluorimeter (Tecan, Switzerland) (Dong et al. 2017).

Assay for protein oxidation and lipid peroxidation

The extracts of livers and kidneys as well as the serum of the mice were prepared as above, and used for the assay of protein oxidation and lipid peroxidation. Protein oxidation was evaluated by the method of Sohal et al. (1993) and Song et al. (2020b). The results were expressed as nanomoles of carbonyl groups per milligram of protein using the excitation coefficient of 22 mM^{-1} cm^{-1} for aliphatic hydrazones.

Malondialdehyde (MDA) is one of the natural substances of lipid peroxidation, and is thus commonly used as a biomarker of lipid peroxidation level. The Lipid Peroxidation MDA Assay Kit (No. S0131S; Beyotime) was used to determinate the generation of MDA in our experiments, and the results were expressed as micromoles per milligram of protein (Okutan et al. 2004).

Measurement of antioxidant enzymes

The extracts of livers and kidneys as well as the serum of the mice were prepared as above, and used for the assay of antioxidant enzymes activity.

Catalase (CAT) activity was detected according to Hsu et al. (2008) and Song et al. (2020b). The specific activity was expressed in terms of micromoles per minute per milligram of protein.

Superoxide dismutase (SOD) activity was dependent on the reduction of nitroblue tetrazolium (WST-8) to water-insoluble blue formazan (Spitz and Oberley 1989). The SOD Assay Kit (No. S0101S; Beyotime) was used to determine total SOD activity. Unit of SOD was expressed as the amount of enzyme that resulted in 50% inhibition of the rate of WST-8 reduction.

Glutathione peroxidase (GPX) activity was detected by the method of Hsu et al. (2008). GPX activity was measured according to the instructions of the GPX Assay Kit (No. S0058; Beyotime).

Assay for effects of rGDF11 on cell viability

rGDF11 expressed in *E.coli* was purified by chromatography on a Ni–NTA resin column as described by Zhou et al. (2019a), and used to test its effect on cell viability. Both the human embryonic lung fibroblast (HELF) cells (a gift of Dr. Bin Wang of the Medical School, Qingdao University) and mouse embryonic

fibroblast 3T3-L1 cells (a gift of Jingfeng Wang of the College of Food Science and Technology, Ocean University of China) were cultured in Dulbecco's modified Eagle media/Nutrient Mixture F-12 (DME/F12) (No: SH30023.01; Hyclone) supplemented with 10% (v/v) fetal bovine serum (FBS) (No: 10099141; Gibco) and antibiotics (100 U/ml penicillin and 100 μg/ml streptomycin) at 37 °C in a humidified atmosphere with 5% CO_2, and in Dulbecco's modified Eagle media (DMEM) (No: 01-052-1ACS; BI) supplemented with 10% FBS (No: 04-001-1ACS; BI) and antibiotics (100 U/ml penicillin and 100 μg/ml streptomycin) at 37 °C in a humidified atmosphere with 5% CO_2, respectively. For both the HELF cells and 3T3-L1 cells, the medium was changed 3 times per week. When the cells reached 90% confluence, they were detached from the plates using a trypsin–EDTA (0.25%) solution (No: SH30042.01; Hyclone) and then suspended in medium containing 10% FBS.

The effects of rGDF11 on the viability of HELF cells and 3T3-L1 cells were evaluated by WST-8 hydrolysis using Cell Counting Kit-8 (No. C0038; Beyotime) as described by Mi et al. (2018). Cells were seeded into 96-well plates (6×10^3 cells/well) in medium supplemented with 10% FBS, and the plates were incubated for 24 h at 37 °C in a humidified incubator with 5% CO_2. The medium was then removed, and the cells were incubated with various concentrations (0, 0.01, 0.05, 0.1, 0.5, and 1 μg/ml) of rGDF11 for 24 h and 48 h. Subsequently, the medium was discarded, and 10 μl of WST-8 was added to each well, followed by incubation for an additional 1 h. Absorbance was measured at 450 nm under a Multiskan MK3 microplate reader. The cells were cultured in triplicate, and samples of at least 3 independent experiments were assayed. The relative cell proliferation ratio results were plotted using the absorbance of non-treated control as 100% activity level. The cell viability was calculated using the following formula: Cell viability (%) = $(A_{rGDF11} - A_{Blank})/(A_{Control} - A_{Blank}) \times 100\%$, in which A_{rGDF11} is the absorbance of cells treated with rGDF11, A_{Blank} is the absorbance of plate, and $A_{Control}$ is the absorbance of cells non-treated.

Assay for effect of inhibitor on induction of antioxidant activity by rGDF11

Cells were seeded into 6-well plates (2×10^5/well) in medium supplemented with 10% FBS, and grown

until they reached confluence (48 h) at 37 °C in a humidified incubator with 5% CO_2. The cells were then treated with or without rGDF11 (0, 0.01, 0.05, 0.1, 0.5 and 1 μg/ml) at 37 °C in a humid atmosphere with 5% CO_2 for 24 h and 48 h. To prepare cell lysates, the cells were detached from the culture plates, and washed three times with cooled PBS. After centrifugation at 300×*g* at 4 °C for 15 min, the pellets were collected and suspended in cooled PBS, and broken by vortexing with glass beads. The lysates were then centrifuged at 12,000×*g* at 4 °C for 15 min, and the supernatants pooled. Protein concentration in the lysates was detected using BCA Protein Assay Kit. The supernatants were used for the activity assay of CAT, SOD and GPX by the specific methods described as above.

For inhibitor studies, cells were seeded and cultured as above. Both the HELF cells and 3T3-L1 cells were pre-incubated with LY2109761 (No: A8464; APExBIO), an inhibitor of TGF-β receptor, at a final concentration of 5 μM for 24 h (Wei et al. 2018; Melisi et al. 2008). After washing twice with PBS to remove cellular debris, the cells were treated with or without rGDF11 (0.5 μg/ml for HELF cells, and 0.1 μg/ml for 3T3-L1 cells) at 37 °C in a humid atmosphere with 5% CO_2 for 24 h and 48 h. Medium was used as control. The cells were then detached from the plates and washed with cooled PBS three times. One part of cells was used for RNAs extraction and cDNAs synthesis for qRT-PCR. For 3T3-L1 cells, the primers used were the same as above. For HELF cells, the primers of human-*cat* (KR711569.1), human-*sod* (NM_000454.5), human-*gpx* (NM_201397.3), and human-*gapdh* (BC025925) were designed using Primer Premier 5.0 program (Supplementary Table 2), and the amplification efficiency of each primer set was also assessed using the HELF cells cDNAs diluted twofold serially (Supplementary Table 3). The other part of cells was used for cellular protein extraction. The cellular proteins extracted were used for assay of antioxidant enzyme activity and Western blotting. For Western blotting assay, the primary antibodies against Smad2/3 (1:1000) (No. 8685 T; Cell Signaling Technology), p-Smad2 (1:1000) (No. 3108 T; Cell Signaling Technology), p-Smad3 (1:1000) (No. 9520 T; Cell Signaling Technology), or β-actin (1:1000) (No. GB12001; Servicebio) were used. The bands were visualized by ECL Western blotting substrate, and analyzed using software Image J. The protein expression levels were normalized to that of β-actin.

Statistical analysis

GraphPad Prism 7 program and software SPSS 13.0 were used to perform statistical analysis. The data regarding survival curves were subjected to the log-rank test. Data from each assay were statistically analyzed by one-way ANOVA, and expressed as the mean ± standard error of the mean (SE of mean). Experiments in this study were all performed in triplicate, and repeated three times except mouse culture. Differences at $p < 0.05$ were considered significant.

Results

Surface display of rGDF11 on *Y. lipolytica*

PCR experiments showed that the positive products were generated only from the gDNAs of yeast cells carrying *gdf11-YlCWP110*, but not from the gDNAs of yeast cells carrying *YlCWP110*. Sequencing analysis of the PCR products verified that *gdf11* was indeed integrated into the gDNAs of *Y. lipolytica* Po1h (data not shown). The immunofluorescent labeling using the His-tag mouse monoclonal antibody as primary antibody and IgG/FITC as second antibody revealed that the green fluorescence was only observed on the surfaces of *Y. lipolytica* cells carrying *gdf11-YlCWP110*, but not on the surfaces of the control cells carrying *YlCWP110* (Fig. 1a), indicating that *gdf11-YlCWP110* was successfully expressed on the yeast cell surface, thus allowing its recognition by the antibodies. This was also corroborated by Western blotting showing that when the GDF11-specific antibody and His-tag monoclonal antibody were used as capture antibody, a major band of approximately 62 kDa (which matched the expected size of mature GDF11 plus His-tag and YlCWP110) was detected in both the total soluble fraction and cell wall fraction of *Y. lipolytica* cells carrying *gdf11-YlCWP110*, but not in the fractions of the cells carrying *YlCWP110* (Fig. 1b and c). These together indicated that GDF11-YlCWP110 fusion protein, or rGDF11, was indeed displayed on the surfaces of *Y. lipolytica* cells.

Next, we performed ELISA to screen a yeast strain with high production of rGDF11. We found that the yield of yeast strain T46 was 2.168 µg rGDF11/g *Y. lipolytica* cells (Fig. 1d and Supplementary Table 1), which was highest among the 100 yeast strains examined. To test if the fusion protein was displayed steadily in T46 strain, it was continuously cultured for 6 generations, and Western blotting was used to detect the protein in the cell cultures from each generation. As shown in Fig. 1e and f, when GDF11-specific antibody and His-tag monoclonal antibody were used as capture antibody, a major band of approximately 62 kDa was always detected in both the total soluble fraction and cell wall fraction of yeast cells from each generation, suggesting a steady display of the fusion protein on T46 yeast cells. Thus, T46 yeast strain was selected for mass culture and used for the following zoopery.

Bioavailability of rGDF11 by oral delivery

Western blotting was used to test the bioavailability of the fusion protein by oral administration in the mice. As shown in Fig. 2, when the GDF11-specific antibody was used as capture antibody, one main band of approximately 45 kDa was detected in the serum of aged male mice prior to the feeding of experimental diets, while at 6 h after feeding of experimental diets two main bands of about 45 and 62 kDa, with some minor bands, were observed in the serum of aged male mice (Fig. 2a). After 1 month feeding with control diets or experimental diets every day, still one main band of approximately 45 kDa was detected in the serum of aged male mice fed with control diets, but two main bands of about 45 and 62 kDa, with some minor bands, were seen in the serum of aged male mice fed
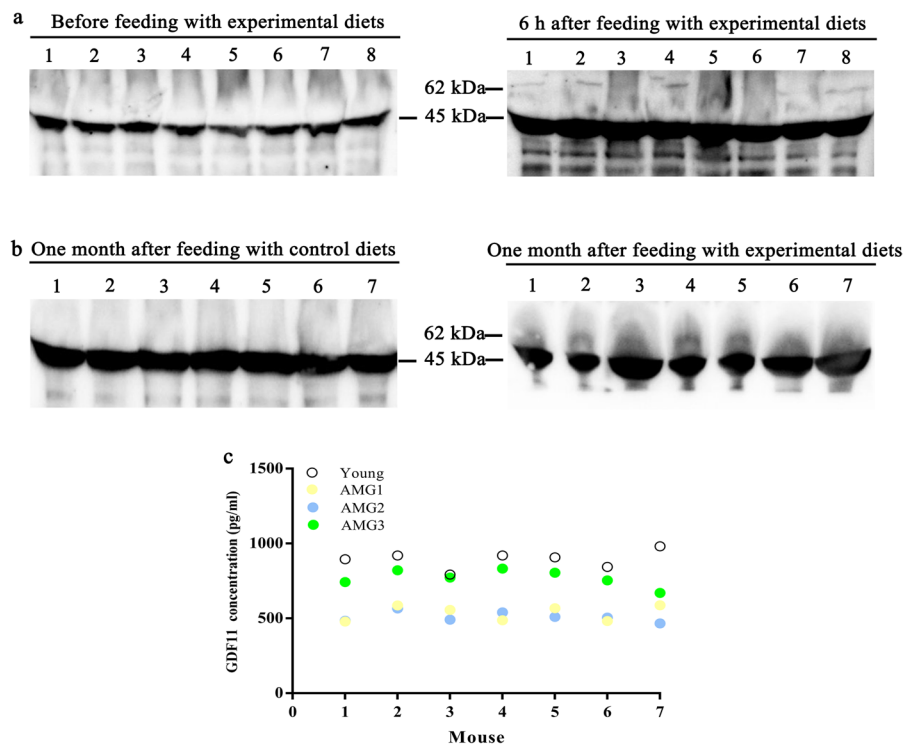

Fig. 2 Bioavailability of rGDF11 by oral delivery. **a** Western blotting of serum of AMG3 group mice, before/after feeding of experimental diets, using mouse anti-GDF11 antibody as the capture antibody (n = 8); **b** Western blotting of serum of AMG2 and AMG3 group mice after feeding with control and experimental diets, using mouse anti-GDF11 antibody as the capture antibody (n = 7). The band of 45 kDa matched the size of natural GDF11 in mice themselves, and the band of 62 kDa corresponded to the size of rGDF11-YlCWP110 fusion protein; **c** The average contents of GDF11 in sera of Young group mice fed with normal diets, AMG1 group mice fed with normal diets, AMG2 group mice fed with control diets and AMG3 group mice fed with experimental diets (n = 7). Date represent mean ± standard deviation (SD)

with experimental diets (Fig. 2b). Moreover, with the aid of standard curve (Supplementary Fig. 2b), we calculated total GDF11 concentration in serum of mice. It revealed that after 1 month feeding, the average GDF11 contents in the serum of young mice fed with normal diets, aged mice (AMG1) fed with normal diets, aged mice (AMG2) fed with control diets and aged mice (AMG3) fed with experimental diets were 895 ± 22.76 pg/ml, 535.6 ± 18.96 pg/ml, 509.4 ± 12.9 pg/ml and 771.6 ± 21.12 pg/ml (Fig. 2c), respectively. GDF11 contents in the serum of mice in AMG1 and AMG2 showed little difference, but compared with young group mice, GDF11 contents in the serum of mice in AMG1 and AMG2 were markedly decreased, confirming that blood GDF11 content declined with age (Zhou et al. 2019a). Notably, GDF11 content in the serum of mice in AMG3 was significantly increased compared with that of mice in AMG1 and AMG2 (Fig. 2c). These together indicated that the displayed rGDF11 fed entered into the blood of aged male mice.

Effects of rGDF11 on body weight, biochemical parameters and lifespan

Figure 3a showed the body weights of aged male mice continuously fed with normal diets, control diets or experimental diets. It revealed that the average body weights of aged mice in AMG1, AMG2 and AMG3 were 38.83 ± 0.10 g, 38.56 ± 0.67 g and 39.13 ± 0.93 g, respectively, at the beginning of the study, which remained stable throughout the trial. In addition, the biochemical parameters of mice, including TP, ALB, GLO, ALT, AST, DBIL, TG, TC, HDL, LDL, BUN, CREA and UA levels showed little difference among mice in AMG1, AMG2 and AMG3 groups (Table 1). These suggested that oral administration of displayed rGDF11 had little influence on the general physiology and health of aged male mice.

Figure 3b showed the survival curves of aged male mice in AMG1, AMG2 and AMG3. The mean and maximum lifespans of mice in AMG1, AMG2 and AMG3 were 30.9 ± 0.1 and 33 ± 1, 30.63 ± 0.64 and 33.67 ± 0.88, 33.1 ± 0.49 and 35.67 ± 0.33 months, respectively. It was found that compared with mice in AMG1 and AMG2, oral administration of rGDF11 considerably prolonged the mean lifespan of mice in
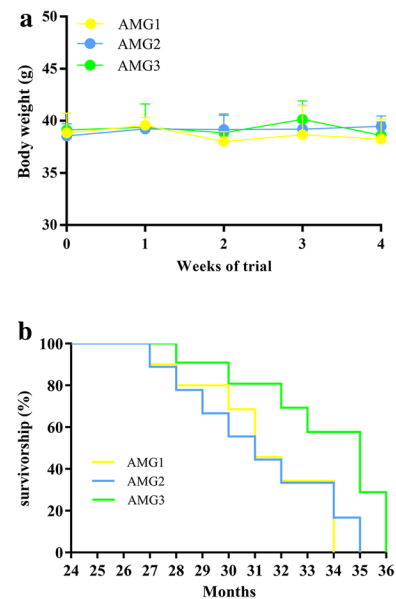
Fig. 3 Effect of rGDF11 on bodyweight and lifespan. **a** Body weight of mice from AMG1, AMG2 and AMG3 groups ($n = 8$). The body weight was measured and recorded every week; **b** The survivorship curves of mice in AMG1, AMG2 and AMG3 groups ($n = 8$). Date represent mean $\pm$ standard deviation (SD)

AMG3 ($p < 0.05$), though their maximum lifespan only slightly increased ($p > 0.05$). These showed that oral administration of displayed rGDF11 had a potential to extend lifespan of aged male mice.

Reduction of aging biomarkers by rGDF11

LF, a marker of cell senescence, was visualized as the bright green-colored auto-fluorescent dots in the cells of liver and kidney of aged mice in AMG1 and AMG2 (Fig. 4a). The green dots in the cells of liver and kidney of mice in AMG1 and AMG2 showed little difference, but they both were remarkably increased (Fig. 4a and b) compared with that of young mice (liver: $0.51 \pm 0.12\%$ vs $3.53 \pm 0.40\%$; $p < 0.01$; kidney: $0.44 \pm 0.04\%$ vs $2.70 \pm 0.21\%$; $p < 0.001$). Of note, compared with mice in AMG1 and AMG2, LF accumulation in the cells of both the liver and kidney of mice in AMG3 was significantly reduced (liver: $1.20 \pm 0.11\%$ vs $3.53 \pm 0.40\%$ or $3.26 \pm 0.72\%$; $p < 0.05$; kidney: $1.00 \pm 0.13\%$ vs $2.70 \pm 0.21\%$ or $2.56 \pm 0.21\%$; $p < 0.01$; Fig. 4a and b). These suggested that oral administration of

Table 1 Biochemical parameters measured in Young, AMG1, AMG2 and AMG3 groups mice

Parameters	AMG1 (n = 7)	AMG2 (n = 7)	AMG3 (n = 7)
TP (g/l)	57.28 ± 0.62	58.1 ± 0.26	57.2 ± 0.85
ALB (g/l)	30.5 ± 0.43	29.2 ± 0.99	29.1 ± 0.23
GLO (g/l)	26.8 ± 0.86	28.9 ± 0.77	28.0 ± 0.66
ALT (U/l)	51.5 ± 9.15	67.0 ± 21.72	56.57 ± 6.96
AST (U/l)	90.7 ± 5.63	115.5 ± 23.87	101.9 ± 5.77
TBIL (μmol/l)	1.9 ± 0.07	2.1 ± 0.44	2.6 ± 0.42
DBIL (μmol/l)	0.5 ± 0.07	0.8 ± 0.20	0.8 ± 0.12
IBIL (μmol/l)	1.3 ± 0.27	1.3 ± 0.24	1.8 ± 0.35
TG (mmol/l)	1.1 ± 0.05	1.1 ± 0.04	1.2 ± 0.16
TC (mmol/l)	3.0 ± 0.21	2.6 ± 0.11	2.8 ± 0.17
HDL (mmol/l)	2.0 ± 0.12	1.8 ± 0.09	1.9 ± 0.13
LDL (mmol/l)	0.43 ± 0.04	0.44 ± 0.02	0.41 ± 0.05
BUN (mmol/l)	7.0 ± 0.67	7.9 ± 0.04	6.7 ± 0.33
CREA (μmol/l)	19.2 ± 1.89	22.4 ± 1.78	22.1 ± 0.93
UA (μmol/l)	254.1 ± 27.34	232.8 ± 12.32	245.3 ± 15.53

[a]Blood was collected at the end of feeding experiment and total protein (TP), albumin (ALB), globulin (GLO), alanine transaminase (ALT), aspartate transferase (AST) activities, total bilirubin (TBIL), direct bilirubin (DBIL), indirect bilirubin (IBIL), triglyceride (TG), total cholesterol (TC), high-density lipoprotein (HDL), low-density lipoprotein (LDL), blood urea nitrogen (BUN), creatinine (CREA) and uric acid (UA) were analyzed as described in "Material and Method"

[b]Values are means ± standard error (SE) of means

rGDF11 reduced the accumulation of LF in aged male mice.

Cellular SA-β-Gal, another widely used biomarker of senescence, is stained blue with X-gal, and the intensity of blue staining represents its activity. As shown in Fig. 4c and d, SA-β-Gal accumulation in the cells of liver and kidney of aged mice in AMG1 and AMG2 showed little difference (liver: $16.02 \pm 1.51\%$ vs $16.89 \pm 1.17\%$; $p > 0.05$; kidney: $44.52 \pm 1.87\%$ vs $44.02 \pm 1.95\%$; $p > 0.05$), which was both markedly higher than that of young mice (liver: $3.77 \pm 0.66\%$ vs $16.89 \pm 0.17\%$ or $16.02 \pm 1.51\%$; $p < 0.001$; kidney: $23.72 \pm 1.68\%$ vs $44.02 \pm 1.95\%$ or $44.52 \pm 1.87\%$; $p < 0.01$). Notably, compared with mice in AMG1 and AMG2, SA-β-Gal contents in the cells of liver and kidney of aged mice in AMG3 were considerably decreased (liver: $9.16 \pm 0.87\%$ vs $16.89 \pm 1.17\%$ or $16.02 \pm 1.51\%$; $p < 0.05$; kidney: $34.46 \pm 2.03\%$ vs $44.02 \pm 1.95\%$ or

$44.52 \pm 1.87\%$; $p < 0.05$) (Fig. 4c and d). These suggested that oral administration of rGDF11 reduced the accumulation of SA-β-Gal in aged male mice.

Reduction of ROS level, protein oxidation and lipid peroxidation by rGDF11

ROS accumulation was also detected in the liver, kidney and serum of aged male mice in AMG1, AMG2 and AMG3. As shown in Fig. 5a and b, little difference was detected in ROS contents in the liver, kidney and serum of mice in AMG1 and AMG2 (liver: 392.0 ± 30.45 vs 368.3 ± 9.53 fluorescence intensity/mg protein; $p > 0.05$; kidney: 104.7 ± 8.01 vs 116.7 ± 12.73 fluorescence intensity/mg protein; $p > 0.05$; serum: 212.3 ± 6.96 vs 211.3 ± 14.1 fluorescence intensity/ml serum; $p > 0.05$), but they were all significantly higher than those of young mice (liver: 268.7 ± 5.90 vs 392.0 ± 30.45 or 368.3 ± 9.53 fluorescence intensity/mg protein; $p < 0.05$; kidney: 60.0 ± 10.12 vs 104.7 ± 8.01 or 116.7 ± 12.73 fluorescence intensity/mg protein; $p < 0.05$; serum: 79.7 ± 6.96 vs 212.3 ± 6.96 or 211.3 ± 14.1 fluorescence intensity/ml serum; $p < 0.001$). Notably, compared with mice in AMG1 and AMG2, ROS levels in the liver, kidney and serum of mice in AMG3 were considerably declined (liver: 295.3 ± 24.37 vs 392.0 ± 30.45 or 368.3 ± 9.53 fluorescence intensity/mg protein; $p < 0.05$; kidney: 47.33 ± 2.96 vs 104.7 ± 8.01 or 116.7 ± 12.73 fluorescence intensity/mg protein; $p < 0.01$; serum: 117.0 ± 22.5 vs 212.3 ± 6.96 or 211.3 ± 14.1 fluorescence intensity/ml serum; $p < 0.05$). These showed that oral administration of displayed rGDF11 decreased ROS level in aged male mice.

Protein oxidation occurs with aging (Sohal and Weindruch 1996). We thus evaluated the levels of protein oxidation (reflected by the accumulation of carbonyl-group) in the liver, kidney and serum of aged male mice in AMG1, AMG2 and AMG3. As shown in Fig. 5c and d, the carbonyl-group levels in the liver, kidney and serum showed little difference between mice in AMG1 and AMG2 (liver: 17.32 ± 0.81 vs 17.62 ± 1.43 nM/mg protein; $p > 0.05$; kidney: 14.04 ± 0.64 vs 14.72 ± 0.24 nM/mg protein; $p > 0.05$; serum: 42.74 ± 2.40 vs 40.43 ± 0.88 nM/ml serum; $p > 0.05$), but they were both remarkably higher than those of young mice (liver: 10.24 ± 0.72
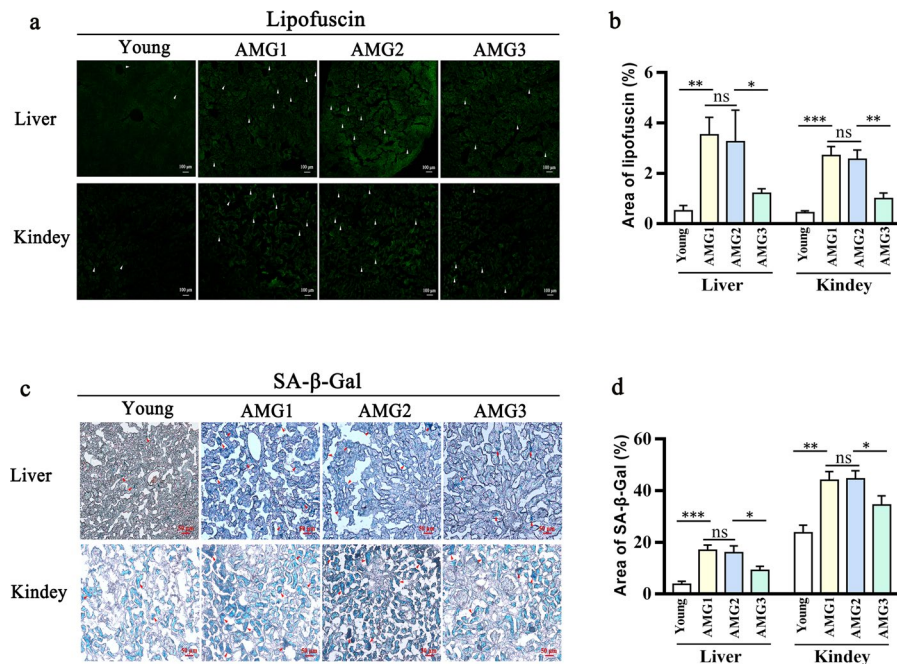
Fig. 4 Reduction of aging biomarkers by rGDF11. **a** LF accumulation in liver and kidney of mice from Young, AMG1, AMG2 and AMG3 groups. *White arrow* heads showed the area of LF dots; **b** statistical analysis of the area occupied by lipofuscin granules in liver and kidney of mice from Young, AMG1, AMG2 and AMG3 groups according to (**a**); **c** SA-β-Gal accumulation in liver and kidney of mice from Young, AMG1, AMG2 and AMG3 groups. *Red arrow* heads indicated the area of SA-β-Gal staining; **d** Statistical analysis of the areas occupied by SA-β-Gal in liver and kidney of mice from Young, AMG1, AMG2 and AMG3 groups according to (**c**). Date represent mean ± standard deviation (SD) (n = 3). *$p < 0.05$; **$p < 0.01$; ***$p < 0.001$; *ns* nonsignificance. Bar is 50 μm and 100 μm

vs 17.62 ± 1.43 or 17.32 ± 0.81 nM/mg protein; $p < 0.01$; kidney: 6.46 ± 0.86 vs 14.72 ± 0.24 or 14.04 ± 0.64 nM/mg protein; $p < 0.01$; serum: 20.28 ± 0.94 vs 40.43 ± 0.88 or 42.74 ± 2.40 nM/ml serum; $p < 0.001$). Of note, compared with mice in AMG1 and AMG2, the carbonyl-group levels in the liver, kidney and serum of mice in AMG3 were significantly decreased (liver: 11.79 ± 1.07 vs 17.32 ± 0.81 or 17.62 ± 1.43 nM/mg protein; $p < 0.05$; kidney: 9.58 ± 0.35 vs 14.04 ± 0.64 or 14.72 ± 0.24 nM/mg protein; $p < 0.001$; serum: 28.11 ± 1.46 vs 42.74 ± 2.40 or 40.43 ± 0.88 nM/ml serum; $p < 0.01$). These indicated that oral administration of displayed rGDF11 retarded the process of protein oxidation in aged male mice.

Lipid peroxidation also happens with aging (Dmitriev and Titov 2010). We thus detected the levels of lipid peroxidation (reflected by the accumulation of MDA) in the liver, kidney and serum of aged male mice in AMG1, AMG2 and AMG3. As shown in Fig. 5e and f, the MDA contents in the liver, kidney

and serum of mice in AMG1 and AMG2 showed little difference (liver: 4.28 ± 0.69 vs 3.77 ± 0.46 μM/mg protein; $p > 0.05$; kidney: 5.25 ± 0.24 vs 5.01 ± 0.41 μM/mg protein; $p > 0.05$; serum: 61.7 ± 1.21 vs 64.46 ± 1.85 μM/ml serum; $p > 0.05$), but they were both markedly higher than those of young mice (liver: 1.35 ± 0.46 vs 3.77 ± 0.46 or 4.28 ± 0.69 μM/mg protein; $p < 0.05$; kidney: 3.22 ± 0.20 vs 5.01 ± 0.41 or 5.25 ± 0.24 μM/mg protein; $p < 0.01$; serum: 32.61 ± 1.27 vs 64.46 ± 1.85 or 61.70 ± 1.21 μM/ml serum; $p < 0.001$). Notably, compared with mice in AMG1 and AMG2, the levels of MDA in the liver, kidney and serum of mice in AMG3 were significantly decreased (liver: 1.52 ± 0.49 vs 4.28 ± 0.69 or 3.77 ± 0.46 μM/mg protein; $p < 0.05$; kidney: 3.67 ± 0.22 vs 5.25 ± 0.24 or 5.01 ± 0.41 μM/mg protein; $p < 0.05$; serum: 53.10 ± 1.46 vs 61.7 ± 1.21 or 64.46 ± 1.85 μM/ml serum; $p < 0.01$). These indicated that oral administration of displayed rGDF11 slowed down the process of lipid peroxidation in aged male mice.

Fig. 5 Reduction of ROS, protein oxidation and lipid peroxidation levels by rGDF11. **a** and **b** ROS accumulation in liver, kidney and serum of mice from Young, AMG1, AMG2 and AMG3 groups; **c** and **d** protein oxidation levels in liver, kidney and serum of mice from Young, AMG1, AMG2 and AMG3 groups; **e** and **f** lipid peroxidation levels in liver, kidney and serum of mice from Young, AMG1, AMG2 and AMG3 groups. Date represent mean ± standard deviation (SD) (n = 3). *$p < 0.05$; **$p < 0.01$; ***$p < 0.001$; *ns* nonsignificance
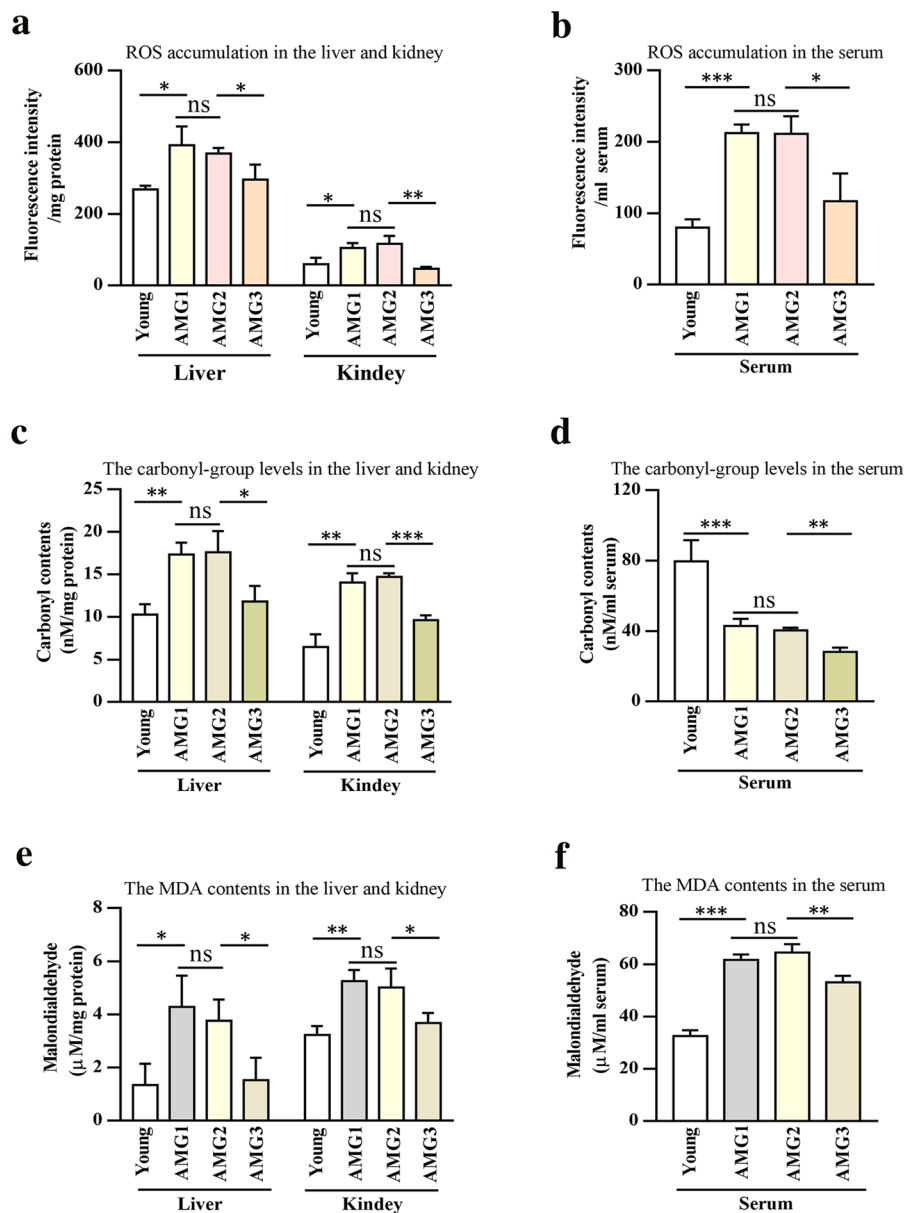
Promotion of antioxidant enzyme activity by rGDF11

As shown in Fig. 6a and b, the CAT activity in the liver, kidney and serum of aged mice in AMG1 and AMG2 was not significantly different from each other (liver: 111.4 ± 5.25 vs 111.8 ± 6.08 μM/min/mg protein, $p > 0.05$; kidney: 88.27 ± 19.52 vs 100.3 ± 6.32 μM/min/mg protein, $p > 0.05$; serum: 115.2 ± 53.30 vs 125.1 ± 14.42 μM/min/ml serum, $p > 0.05$), but the activity of CAT in the three tissues of mice in AMG1 and AMG2

was all markedly lower than that of young mice (liver: 111.4 ± 5.25 vs 209.0 ± 6.00 μM/min/mg protein, $p < 0.001$; kidney: 88.3 ± 19.52 vs 327.0 ± 19.42 μM/min/mg protein, $p < 0.001$; serum: 125.1 ± 14.42 vs 280.2 ± 15.83 μM/min/ml serum, $p < 0.01$). Compared with mice in AMG1 and AMG2, the activity of CAT in the liver, kidney and serum of aged mice in AMG3 was significantly increased (liver: 111.4 ± 5.25 or 111.8 ± 6.08 vs 148.9 ± 9.19 μM/min/mg protein, $p < 0.05$; kidney: 88.27 ± 19.52 or 100.3 ± 6.32 vs 198.6 ± 9.67 μM/
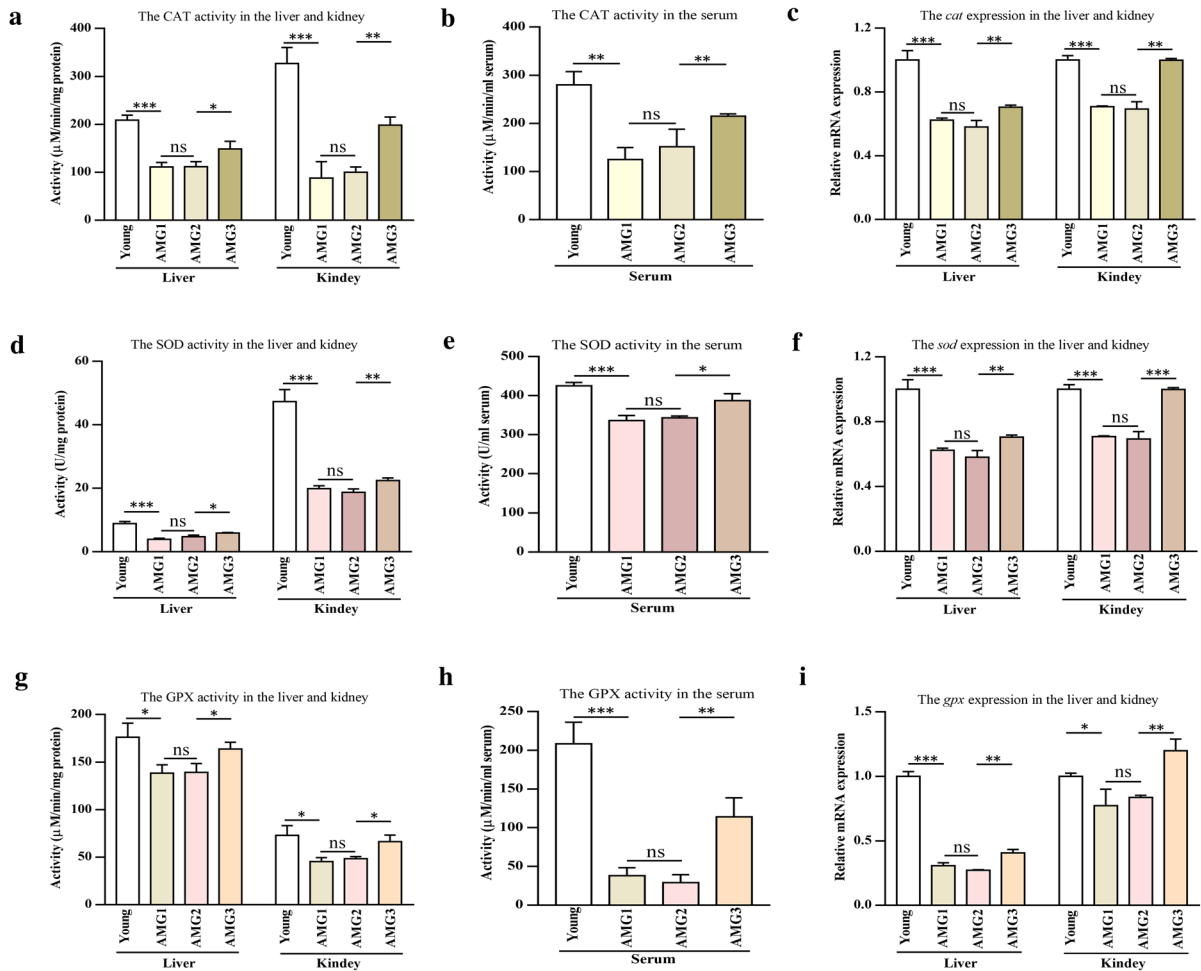
Fig. 6 Promotion of antioxidant enzyme activity by rGDF11. **a** and **b** The activity of CAT in liver, kidney and serum of mice from Young, AMG1, AMG2 and AMG3 groups; **c** the mRNA level of *cat* in liver and kidney of mice from Young, AMG1, AMG2 and AMG3 groups; **d** and **e** the activity of SOD in liver, kidney and serum of mice from Young, AMG1, AMG2 and AMG3 groups; **f** the mRNA level of *sod* in liver and kid-ney of mice from Young, AMG1, AMG2 and AMG3 groups; **g** and **h** the activity of GPX in liver, kidney and serum of mice from Young, AMG1, AMG2 and AMG3 groups; **i** the mRNA level of *gpx* in liver and kidney of mice from Young, AMG1, AMG2 and AMG3 groups. Date represent mean ± standard deviation (SD) (n = 3). *$p < 0.05$; **$p < 0.01$; ***$p < 0.001$; *ns* nonsignificance

min/mg protein, $p < 0.01$; serum: 115.2 ± 53.30 or 125.1 ± 14.42 vs 214.7 ± 2.95 µM/min/ml serum, $p < 0.01$). In accordance, the expression of *cat* in the liver and kidney of mice in AMG3 was also considerably higher than that in the same tissues of mice in AMG1 and AMG2 ($p < 0.01$). The expression of *cat* in the liver and kidney of mice in AMG1 and AMG2 showed little difference ($p > 0.05$), but was remarkably lower than that in the same tissues of young mice ($p < 0.001$; Fig. 6c). These together indicated that oral administration

of displayed rGDF11 promoted both the activity of CAT and its gene expression in aged male mice.

The SOD activity in the liver, kidney and serum of aged mice in AMG1 and AMG2 showed lit-tle difference between each other (liver: 3.93 ± 0.21 vs 4.73 ± 0.31 U/mg protein, $p > 0.05$; kidney: 19.79 ± 0.54 vs 18.69 ± 0.61 U/mg protein, $p > 0.05$; serum: 336.2 ± 7.44 vs 343.1 ± 2.68 U/ml serum, $p > 0.05$), but the activity of SOD in the three tissues of mice in AMG1 and AMG2 was all mark-edly lower than that of young mice (liver: 3.93 ± 0.21

or 4.73 ± 0.31 vs 8.88 ± 0.41 U/mg protein, $p < 0.001$; kidney: 19.79 ± 0.54 or 18.69 ± 0.61 vs 47.3 ± 2.20 U/mg protein, $p < 0.001$; serum: 336.2 ± 7.44 or 343.1 ± 2.68 vs 425.4 ± 5.04 U/ml serum, $p < 0.001$). Compared with mice in AMG1 and AMG2, the activity of SOD in the liver, kidney and serum of aged mice in AMG3 was remarkably increased (liver: 3.93 ± 0.21 or 4.73 ± 0.31 vs 5.94 ± 0.06 U/mg protein, $p < 0.05$; kidney: 18.69 ± 0.61 or 19.79 ± 0.54 vs 22.37 ± 0.48 U/mg protein, $p < 0.01$; serum: 343.1 ± 2.68 or 336.2 ± 7.44 vs 387.1 ± 10.42 U/ml serum, $p < 0.05$; Fig. 6d and e). Consistently, the expression of *sod* in the liver and kidney of mice in AMG3 was also markedly higher than that in the same tissues of mice in AMG1 and AMG2 ($p < 0.01$). The expression of *sod* in the liver and kidney of mice in AMG1 and AMG2 was closely similar to each other ($p > 0.05$), but was considerably lower than that in the same tissues of young mice ($p < 0.001$; Fig. 6f). These together showed that oral administration of displayed rGDF11 promoted both the activity of SOD and its gene expression in aged male mice.

The GPX activity in the liver, kidney and serum of aged mice in AMG1 and AMG2 was not different from each other (liver: 138.4 ± 5.02 vs 139.1 ± 5.40 μM/min/mg protein, $p > 0.05$; kidney: 45.41 ± 2.44 vs 48.45 ± 1.25 μM/min/mg protein, $p > 0.05$; serum: 29.06 ± 6.02 vs 38.03 ± 6.09 μM/min/ml serum, $p > 0.05$), but the activity of GPX in the three tissues of mice in AMG1 and AMG2 was all markedly lower than that of young mice (liver: 138.4 ± 5.02 or 139.1 ± 5.40 vs 176.3 ± 8.52 μM/min/mg protein, $p < 0.05$; kidney: 45.41 ± 2.44 or 48.45 ± 1.25 vs 72.9 ± 5.87 μM/min/mg protein, $p < 0.05$; serum: 29.06 ± 6.02 or 38.03 ± 6.09 vs 208.5 ± 16.11 μM/min/ml serum, $p < 0.001$). Compared with mice in AMG1 and AMG2, the activity of GPX in the liver, kidney and serum of aged mice in AMG3 was significantly increased (liver: 138.4 ± 5.02 or 139.1 ± 5.40 vs 162.8 ± 4.07 μM/min/mg protein, $p < 0.05$; kidney: 45.41 ± 2.44 or 48.45 ± 1.25 vs 66.32 ± 4.06 μM/min/mg protein, $p < 0.05$; serum: 29.06 ± 6.02 or 38.03 ± 6.09 vs 114.0 ± 14.38 μM/min/ml serum, $p < 0.01$; Fig. 6g and h). In agreement, the expression of *gpx* in the liver and kidney of mice in AMG3 was markedly higher than that in the same tissues of mice in AMG1 and AMG2 ($p < 0.01$). The

expression of *gpx* in the liver and kidney of mice in AMG1 and AMG2 was not different from each other ($p > 0.05$), but was considerably lower than that in the same tissues of young mice ($p < 0.001$; Fig. 6i). These together showed that oral administration of displayed rGDF11 promoted both the activity of GPX and its gene expression in aged male mice.

Promotion of antioxidant activity by rGDF11 via Smad2/3 pathway

As shown in Supplementary Fig. 3, rGDF11 had little influence on the growth of HELF cells and 3T3-L1 cells at a concentration as high as 1 μg/ml. Both HELF and 3T3-L1 cells were then incubated with different concentrations (0, 0.01, 0.05, 0.1, 0.5 and 1 μg/ml) of rGDF11 for 24 h and 48 h, and the cell lysates were prepared and used for antioxidant enzyme activity assay. It was found that at the concentration ranging from 0.01 to 0.5 μg/ml, rGDF11 was able to increase the antioxidant enzyme activities of both CAT and SOD as well as GPX in both the HELF cells and 3T3-L1 cells in a dose-dependent manner (Fig. 7). The concentrations of 0.1 and 0.5 μg/ml were then chosen for the inhibitor experiments.

As shown in Fig. 8, the inhibitor LY2109761 was able to markedly reduce the activities of CAT, SOD and GPX in both the HELF cells and 3T3-L1 cells cultured in the presence or absence of rGDF11. LY2109761 was also able to significantly decrease the expression of *cat*, *sod* and *gpx* in both the cells cultured in the presence or absence of rGDF11. These showed that promotion of antioxidant activity by rGDF11 was suppressed by the inhibitor LY2109761.

Interestingly, rGDF11 was found to have little influence on the total Smad2/3 levels in both the HELF cells and 3T3-L1 cells, but their contents of p-Smad2 and p-Smad3 as well as the activities of p-Smad2 (expressed by p-Smad2/Smad2/3) and p-Smad3 (expressed by p-Smad3/Smad2/3) were significantly increased by rGDF11 (Fig. 9), suggesting that rGDF11 acted through phosphorylation of the intracellular signaling proteins SMAD2 and SMAD3. By contrast, although LY2109761 showed little influence on the total Smad2/3 levels in both the HELF cells and 3T3-L1 cells cultured in the presence or absence of rGDF11, their contents of p-Smad2 and p-Smad3 as well as the activities of p-Smad2 and p-Smad3 were markedly decreased by treatment
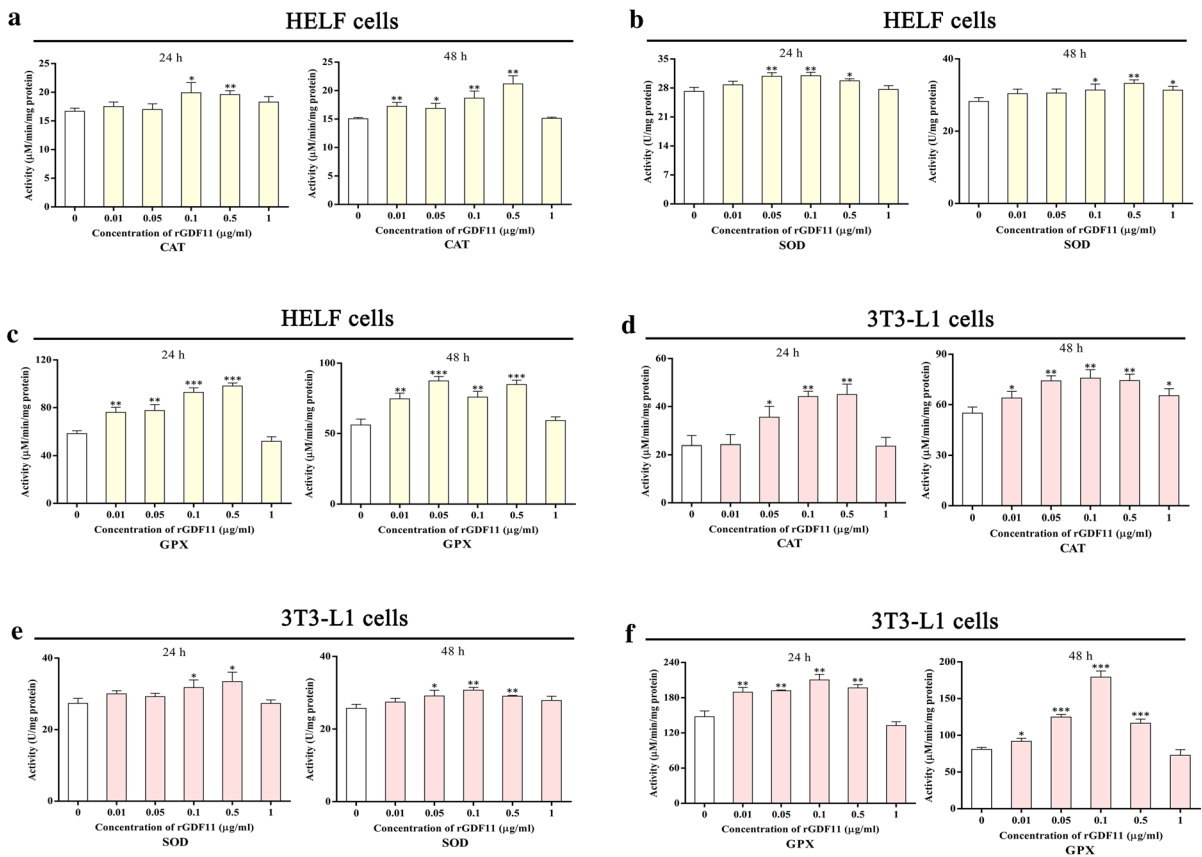
Fig. 7 Promotion of antioxidant enzyme activity of HELF cells and 3T3-L1 cells by rGDF11. **a–c** The CAT, SOD and GPX activities of HELF cells treated with different concentration of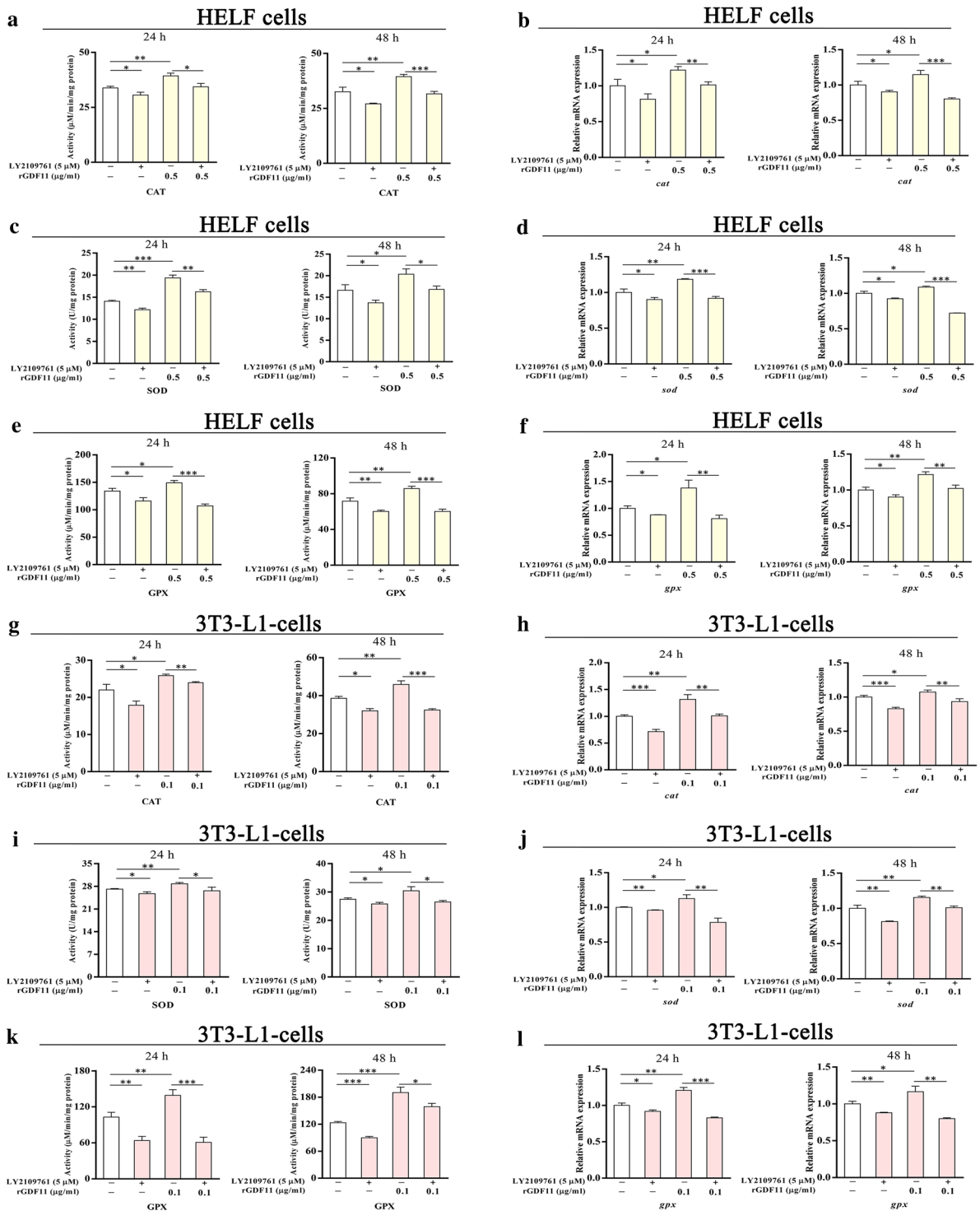 rGDF11 at 24 h and 48 h; **d–f** the CAT, SOD and GPX activities of 3T3-L1 cells treated with different concentration of rGDF11 at 24 h and 48 h. Date represent mean ± standard deviation (SD) (n = 3). *$p < 0.05$; **$p < 0.01$; ***$p < 0.001$

with LY2109761 (Fig. 9). These data together showed rGDF11 promoted antioxidant activity by activation of the Smad2/3 signaling pathway.

Discussion

Since the discovery of GDF11 as a "youth factor" (Loffredo et al. 2013), it has become a "hot" molecule in the field of anti-aging study. Yet it is still controversial over the age-related change in concentration of GDF11 and its role in the genesis of rejuvenation conditions. With the aid of a highly specific anti-GDF11 antibody (sc-81952, Santa Cruz), here we show that GDF11 concentration declines with age in male mice, confirming the results of ours and others that blood GDF11 abundance reduces with age in both

fish and mouse as well as humans (Loffredo et al. 2013; Andersen and Lim 2014; Brack 2013; Hall 2014; Kaiser 2015; Katsimpardi et al. 2014; Zhou et al. 2016, 2019a). We also show the bioavailability of yeast-displayed rGDF11 by oral delivery in aged male mice. Importantly, we demonstrate that dietary intake of displayed rGDF11 delays the occurrence and development of age-related biomarkers such as LF and SA-β-Gal. Moreover, to some extent, dietary intake of displayed rGDF11 also prolongs the lifespan of aged male mice, though it needs testing with more mice (in our study only 8 mice were tested because of the limitation of yeast production). Altogether these data provide additional evidences that GDF11 has rejuvenation activity, capable of reversing aging (Loffredo et al. 2013; Katsimpardi et al. 2014; Zhou et al. 2019a, b; Sinha et al. 2014). As for the controversy

◄**Fig. 8** LY2109761 suppressed the antioxidant enzyme activity and expression in the presence or absence of rGDF11. **a**, **c** and **e** The CAT, SOD and GPX activities of HELF cells treated with LY2109761 or rGDF11 at 24 h and 48 h; **b**, **d** and **f** the *cat*, *sod* and *gpx* mRNA expressions of HELF cells treated with LY2109761 or rGDF11 at 24 h and 48 h; **g**, **i** and **k** the CAT, SOD and GPX activities of 3T3-L1 cells treated with LY2109761 or rGDF11 at 24 h and 48 h; **h**, **j** and **l** the *cat*, *sod* and *gpx* mRNA expressions of 3T3-L1 cells treated with LY2109761 or rGDF11 at 24 h and 48 h. Date represent mean ± standard deviation (SD) (n = 3). *$p < 0.05$; **$p < 0.01$; ***$p < 0.001$

over the concentration and role of GDF11 in aging, it may be due to either the selectivity of the tests used to measure GDF11 or the activity of GDF11 from various commercially available sources or both (Kaiser 2015).

"Free radical damage theory" initially proposed by Denham Harman (1956) is one of the most studied and widely accepted conjectures on the molecular basis of aging process. Our previous studies have suggested that GDF11 performs its anti-aging activity via the action of antioxidant system in both fish and mice (Zhou et al. 2019a, b), but how GDF11 induces the enhancement of antioxidant system is unknown. In this study, we demonstrate once again that dietary intake of displayed rGDF11 enhances the activities of anti-oxidant enzymes, including CAT, GPX and SOD, reduces the levels of ROS, and slows down the protein oxidation and lipid peroxidation. Especially, we show for the first time that rGDF11 enhances the activities of CAT, SOD and GPX through activation of the Smad2/3 signaling pathway. Therefore, it is highly likely that the chain of reaction for GDF11 executing its rejuvenation activity is that GDF11 induces generation of antioxidant enzymes (CAT, SOD and GPX), which directly results in reduction of ROS levels, which then decelerates protein oxidation, lipid peroxidation and possibly LF and SA-β-Gal development, which in turn extends lifespan of aged mice.

Another important point we have to point out is that although our study is limited to aged male mice, the anti-aging effects of GDF11 are expected similarly applicable for female mice. The "free radical damage theory" suggests that excess ROS can cause oxidative damage to the macromolecules of cells, including DNA, RNA, proteins, carbohydrates and lipids (Beckman and Ames 1998; Giordano et al. 2013), thus it is applicable for all multicellular organisms at cellular level (Beckman and Ames 1998; Finkel and Holbrook 2000; Larsen 1993; Meng et al. 2017). As mentioned above, rGDF11 exerts its rejuvenation and anti-aging activity through suppression of ROS production, which is thus believed to equally benefit to both male and female mice.

Yeast cell surface display technology has been regarded as a powerful tool with interesting applications in cell adhesion, molecular recognition, immobilized biocatalyst, bioconversion, bioremediation, change of cell function, signal transduction, biosensor and live vaccine development (Becker et al. 2004; Lee et al. 2006; Ueda and Tanaka 2000; Zhu et al. 2006). Many proteins such as enhanced green fluorescent protein (EGFP), hemolysin, alkaline protease, methyl parathion hydrolase (MPH) and silicatein have been displayed on *Y. lipolytica* cells surface by the glycosylphosphatidyl inositol-anchor-fusion expression system (Yue et al. 2008; Ni et al. 2009; Wang et al. 2012, 2020), and the proteins displayed all show normal or even stronger activities. Using the same expression system, GDF11 is successfully displayed on the surfaces of yeast *Y. lipolytica* in this study, and shown to have rejuvenation/anti-aging activity. Given that *E. coli* is an opportunistic pathogen, people are often worried about application of its products. By contrast, rGDF11 displayed on the surfaces of *Y. lipolytica* cells with GRAS is quite safe, and can be accepted easily by the public, which will certainly benefit its therapeutic application in the future.

In summary, our study shows that GDF11 displayed on the surface of *Y. lipolytica* exibits anti-aging activity in aged male mice. It also shows that displayed rGDF11 promotes activity of antioxidant enzymes via activation of Smad2/3 signaling pathway. Additionally, it provides a simple and safe route for delivery of recombinant GDF11, facilitating its therapeutic application.
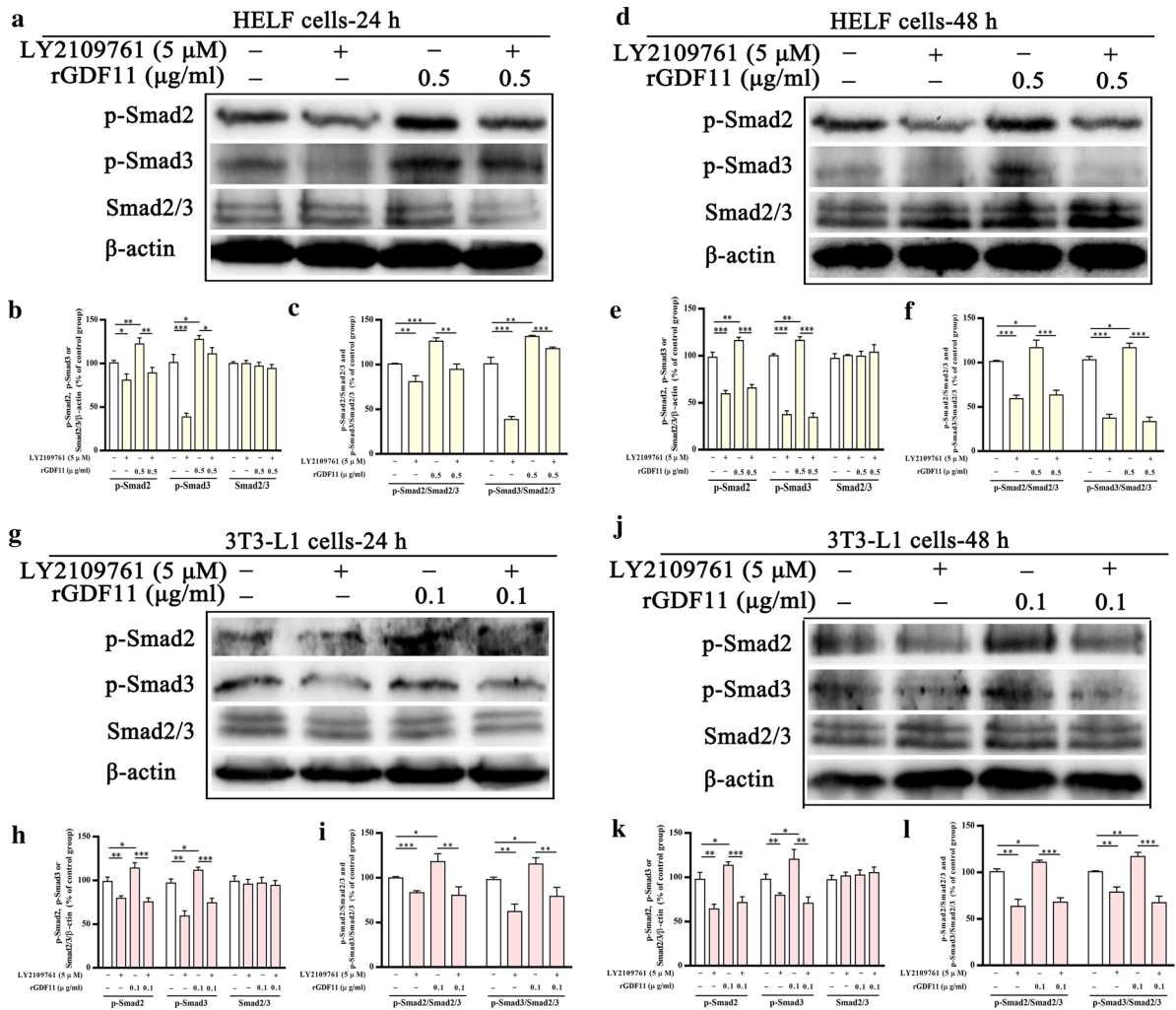
Fig. 9 LY2109761 suppressed Smad2/3 signaling pathway in the presence or absence of rGDF11. **a** and **d** The expressions of Smad2/3, p-Smad2 and p-Smad3 in HELF cells treated with LY2109761 or rGDF11 at 24 h and 48 h were analyzed through western blotting. β-actin was chosen as the internal control for normalization; **b** and **e** the expressions of Smad2/3, p-Smad2 and p-Smad3 in HELF cells treated with LY2109761 or rGDF11 at 24 h and 48 h were calculated from the densities of the low bands and normalized to the expression in HELF control cells according to Fig. 8a and d; **c** and **f** the ratio of p-Smad2/Smad2/3 and p-Smad3/Smad2/3 in HELF cells treated with LY2109761 or rGDF11 at 24 h and 48 h were calculated according to Fig. 8b and e; **g** and **j** the expres-

sions of Smad2/3, p-Smad2 and p-Smad3 in 3T3-L1 cells treated with LY2109761 or rGDF11 at 24 h and 48 h were analyzed through western blotting. β-actin was chosen as the internal control for normalization; **h** and **k** the expressions of Smad2/3, p-Smad2 and p-Smad3 in 3T3-L1 cells treated with LY2109761 or rGDF11 at 24 h and 48 h were calculated from the densities of the low bands and normalized to the expression in 3T3-L1 control cells according to Fig. 8g and j; **i** and **l** the ratio of p-Smad2/Smad2/3 and p-Smad3/Smad2/3 in 3T3-L1 cells treated with LY2109761 or rGDF11 at 24 h and 48 h were calculated according to Fig. 8h and k. Date represent mean ± standard deviation (SD) (n = 3). *$p < 0.05$; **$p < 0.01$; ***$p < 0.001$

Data availability All data generated or analysed during this study are included in this published article (and its supplementary information files).

Declarations

Conflict of interest No competing financial interests exist.

References

Andersen RE, Lim DA (2014) An ingredient for the elixir of youth. Cell Res 24:1381–1382

Andersson O, Reissmann E, Ibañez CF (2006) Growth differentiation factor 11 signals through the transforming growth factor-beta receptor ALK5 to regionalize the anterior-posterior axis. EMBO Rep 7:831–837

Becker S, Schmoldt HU, Adams TM, Wilhelm S, Kolmar H (2004) Ultrahigh-throughput screening based on cell-surface display and fluorescence-activated cell sorting for the identification of novel biocatalysts. Curr Opin Biotechnol 15:323–329

Beckman KB, Ames BN (1998) The free radical theory of aging matures. Physiol Rev 78:547–581

Borsenberger V, Onésime D, Lestrade D et al (2018) Multiple parameters drive the efficiency of CRISPR/Cas9 induced gene modifications in *Yarrowia lipolytica*. J Mol Biol 430:4293–4306

Brack AS (2013) Ageing of the heart reversed by youthful systemic factors! EMBO J 32:2189–2190

Cherf GM, Cochran JR (2015) Applications of yeast surface display for protein engineering. Methods Mol Biol 1319:155–175

Dmitriev LF, Titov VN (2010) Lipid peroxidation in relation to ageing and the role of endogenous aldehydes in diabetes and other age-related diseases. Ageing Res Rev 9:200–210

Dong Y, Cui P, Li Z, Zhang S (2017) Aging asymmetry: systematic survey of changes in age-related biomarkers in the annual fish *Nothobranchius guentheri*. Fish Physiol Biochem 43:309–319

Egerman MA, Cadena SM, Gilbert JA et al (2015) GDF11 increases with age and inhibits skeletal muscle regeneration. Cell Metab 22:164–174

Finkel T, Holbrook NJ (2000) Oxidants, oxidative stress and the biology of ageing. Nature 408:239–247

Fujitsuka N, Asakawa A, Morinaga A et al (2016) Increased ghrelin signaling prolongs survival in mouse models of human aging through activation of sirtuin1. Mol Psychiatry 21:1613–1623

Giordano S, Darley-Usmar V, Zhang JH (2013) Autophagy as an essential cellular antioxidant pathway in neurodegenerative disease. Redox Biol 2:82–90

Hall SS (2014) Young blood. Science 345:1234–1237

Harman D (1956) Aging: a theory based on free radical and radiation chemistry. J Gerontol 11:298–300

Hsu CY, Chiu YC, Hsu WL, Chan YP (2008) Age-related markers assayed at different developmental stages of the annual fish *Nothobranchius rachovii*. J Gerontol A Biol Sci Med Sci 63:1267–1276

Hunsche C, Hernandez O, De la FM (2016) Impaired immune response in old mice suffering from obesity and premature immunosenescence in adulthood. J Gerontol A Biol Sci Med Sci 71:983–991

Kaiser J (2015) Regenerative medicine. 'Rejuvenating' protein doubted. Science 348:849

Katsimpardi L, Litterman NK, Schein PA et al (2014) Vascular and neurogenic rejuvenation of the aging mouse brain by young systemic factors. Science 344:630–634

Kunstyr I, Leuenberger HG (1975) Gerontological data of C57BL/6J mice. I. Sex differences in survival curves. J Gerontol 30:157–162

Larsen R (1993) Hypoxia. Introduction. Anasth Intensiv Notf 28:30–31

Lee HW, Lee SH, Park KJ et al (2006) Construction and characterization of a pseudo-immune human antibody library using yeast surface display. Biochem Biophys Res Commun 346:896–903

Lebrun JJ, Takabe K, Chen Y, Vale W (1999) Roles of pathway-specific and inhibitory Smads in activin receptor signaling. Mol Endocrinol 13:15–23

Liu T, Qi H, Ma L et al (2015) Resveratrol attenuates oxidative stress and extends life span in the annual fish *Nothobranchius guentheri*. Rejuvenation Res 18:225–233

Lim Y, Zhong JH, Zhou XF (2015) Development of mature BDNF-specific sandwich ELISA. J Neurochem 134:75–85

Loffredo FS, Steinhauser ML, Jay SM, Gannon J, Pancoast JR et al (2013) Growth differentiation factor 11 is a circulating factor that reverses age-related cardiac hypertrophy. Cell 153:828–839

Madzak C, Gaillardin C, Beckerich JM (2004) Heterologous protein expression and secretion in the non-conventional yeast *Yarrowia lipolytica*: a review. J Biotechnol 109:63–81

Markofsky J, Perlmutter A (1973) Growth differences in subgroups of varying longevities in a laboratory population of the male annual cyprinodont fish, *Nothobranchius guentheri* (Peters). Exp Gerontol 8:65–73

McPherron AC, Lee S, Lawler AM (1999) Regulation of anterior/posterior patterning of the axial skeleton by growth/differentiation factor 11. Nat Genet 22:260–264

Melisi D, Ishiyama S, Sclabas MG et al (2008) LY2109761, a novel transforming growth factor β receptor type I and type II dual inhibitor, as a therapeutic approach to suppressing pancreatic cancer metastasis. Mol Cancer Ther 7:829–840

Meng FX, Hou JM, Sun TS (2017) Effect of oxidative stress induced by intracranial iron overload on central pain after spinal cord injury. J Orthop Surg Res 12:24

Mi B, Liu J, Liu Y et al (2018) The designer antimicrobial peptide A-hBD-2 facilitates skin wound healing by stimulating keratinocyte migration and proliferation. Cell Physiol Biochem 51:647–663

Moon HY, Van LT, Cheon SA et al (2013) Cell-surface expression of *Aspergillus saitoi*-derived functional α-1,2-mannosidase on *Yarrowia lipolytica* for glycan remodeling. J Microbiol 51:506–514

Ni XM, Yue LX, Chi ZM et al (2009) Alkaline protease gene cloning from the marine yeast *Aureobasidium pullulans* HN2-3 and the protease surface display on *Yarrowia lipolytica*. Mar Biotechnol 11:81–89

Okutan H, Savas C, Delibas N (2004) The antioxidant effect of melatonin in lung injury after aortic occlusion-reperfusion. Interact Cardiov Thorac Surg 3:519–522

Ozek C, Krolewski RC, Buchanan SM, Rubin LL (2018) Growth differentiation factor 11 treatment leads to neuronal and vascular improvements in the hippocampus of aged mice. Sci Rep 8:17293

Paul Oh S, Yeo CY, Lee Y et al (2002) Activin type IIA and IIB receptors mediate Gdf11 signaling in axial vertebral patterning. Genes Dev 16:2749–2754

Patel K, Amthor H (2005) The function of Myostatin and strategies of Myostatin blockade-new hope for therapies aimed at promoting growth of skeletal muscle. Neuromuscul Disord 15:117–126

Poggioli T, Vujic A, Yang P, Macias-Trevino C, Uygur A et al (2016) Circulating growth differentiation factor 11/8 levels decline with age. Circ Res 118:29–37

Pringle JR, Adams AE, Drubin DG, Haarer BK (1991) Immunofluorescence methods for yeast. Methods Enzymol 194:565–602

Rochette L, Zeller M, Cottin Y, Vergely C (2015) Growth and differentiation factor 11 (GDF11): functions in the regulation of erythropoiesis and cardiac regeneration. Pharmacol Ther 156:26–33

Rodgers BD, Eldridge JA (2015) Reduced circulating GDF11 is unlikely responsible for age-dependent changes in mouse heart, muscle, and brain. Endocrinology 156:3885–3888

Schafer MJ, Atkinson EJ, Vanderboom PM et al (2016) Quantification of GDF11 and myostatin in human aging and cardiovascular disease. Cell Metab 23:1207–1215

Smith SC, Zhang XX, Zhang XY et al (2015) GDF11 does not rescue aging-related pathological hypertrophy. Circ Res 117:926–932

Sinha M, Jang YC, Oh J et al (2014) Restoring systemic GDF11 levels reverses age-related dysfunction in mouse skeletal muscle. Science 344:649–652

Spitz DR, Oberley LW (1989) An assay for superoxide dismutase activity in mammalian tissue homogenates. Anal Biochem 179:8–18

Sohal RS, Weindruch R (1996) Oxidative stress, caloric restriction, and aging. Science 273:59–63

Sohal RS, Agarwal S, Dubey A, Orr WC (1993) Protein oxidative damage is associated with life expectancy of houseflies. Proc Natl Acad Sci USA 90:7255–7259

Song LL, Yuan JS, Ni SS et al (2020a) Enhancement of adaptive immune responses of aged mice by dietary intake of β-glucans, with special emphasis on anti-aging activity. Mol Immunol 117:160–167

Song LL, Zhou Y, Ni SS et al (2020b) Dietary intake of β-glucans can prolong lifespan and exert an antioxidant action of aged fish *Nothobranchius guentheri*. Rejuvenation Res 23:293–301

Ueda M, Tanaka A (2000) Genetic immobilization of proteins on the yeast cell surface. Biotechnol Adv 18:121–140

Walker RG, Poggioli T, Katsimpardi L et al (2016) Biochemistry and biology of GDF11 and myostatin: similarities, differences, and questions for future investigation. Circ Res 118:1125–1141

Wang XX, Chi Z, Ru SG, Chi ZM (2012) Genetic surface-display of methyl parathion hydrolase on *Yarrowia lipolytica* for removal of methyl parathion in water. Biodegradation 23:763–774

Wang HY, Wang ZZ, Liu GL et al (2020) Genetical surface display of silicatein on *Yarrowia lipolytica* confers living and renewable biosilica yeast hybrid materials. ACS Omega 5:7555–7566

Wei G, Xu QQ, Liu L et al (2018) LY2109761 reduces TGF-β1-induced collagen production and contraction in hypertrophic scar fibroblasts. Arch Dermatol Res 310:615–623

Xuan JM, Fournier P, Gaillardin C (1988) Cloning of the LYS5 gene encoding saccharopine dehydrogenase from the yeast *Yarrowia lipolytica* by target integration. Curr Genet 14:15–21

Yang YJ, Yang Y, Wang X, Du J, Hou JN et al (2017) Does growth differentiation factor 11 protect against myocardial ischaemia/reperfusion injury? A hypothesis. J Int Med Res 45:1629–1635

Yue LX, Chi ZM, Wang L et al (2008) Construction of a new plasmid for surface display on cells of *Yarrowia lipolytica*. J Microbiol Methods 72:116–123

Zhou Y, Jiang Z, Harris EC et al (2016) Circulating concentrations of growth differentiation factor 11 are heritable and correlate with life span. J Gerontol A Biol Sci Med Sci 71:1560–1563

Zhou Y, Ni SH, Song LL et al (2019a) Late-onset administration of GDF11 extends life span and delays development of age-related markers in the annual fish *Nothobranchius guentheri*. Biogerontology 20:225–239

Zhou Y, Song LL, Ni SH et al (2019b) Administration of rGDF11 retards the aging process in male mice via action of anti-oxidant system. Biogerontology 20:433–443

Zhu KL, Chi ZM, Li J (2006) The surface display of haemolysin from *Vibrio harveyi* on yeast cells and their potential applications as live vaccine in marine fish. Vaccine 24:6046–6052

Publisher's Note Springer Nature remains neutral with regard to jurisdictional claims in published maps and institutional affiliations.